

Cite this: *Sustainable Food Technol.*,  
2025, 3, 2088

# Neem leaf-derived carbon dot-embedded chitosan-based active films: a sustainable approach to prolong the shelf life of prawns

Ajitkumar Appayya Hunashyal,<sup>a</sup> Saraswati P. Masti,<sup>b</sup>  \*<sup>a</sup> Lingaraj Kariyappa Kurabetta,<sup>b</sup> Manjushree Nagaraj Gunaki,<sup>a</sup> Suhasini Madihalli,<sup>a</sup> Jennifer P. Pinto,<sup>b</sup> Manjunath B. Megalamani,<sup>c</sup>  Bothe Thokchom,<sup>d</sup> Ramesh Babu Yarajarla <sup>d</sup> and Ravindra B. Chougale<sup>e</sup>

In response to growing environmental concerns and the demand for sustainable, functional food packaging, this study adopts a green nanotechnology approach by utilising phytochemically rich neem leaves to produce fluorescent and bioactive carbon dots (NLCDs). The NLCDs, prepared *via* a one-pot hydrothermal route, formed quasi-spherical nanostructures (~8 nm) with abundant oxygen- and nitrogen-containing surface functional groups. These confer a strong electron-donating capacity, enabling the efficient scavenging of reactive oxygen species, while their quantum confinement and surface defect states underpin an excitation-dependent blue fluorescence (450 nm) and UV-vis absorption at 220 and 270 nm. When incorporated into a chitosan/polyvinyl alcohol (CP) matrix *via* solvent casting, the small size and uniform dispersion of NLCDs promoted strong hydrogen bonding and interfacial compatibility, as confirmed by FTIR, XRD, and SEM analyses. These reduced the polymer chain mobility, increasing the tensile strength by 66% (43.7 MPa) and enhancing the UV-blocking performance (93% attenuation at 280 nm). Antioxidant activity reached 82% (DPPH) and 77% (H<sub>2</sub>O<sub>2</sub>), attributable to the synergistic effects of NLCDs and the CP matrix. The films demonstrated potent antibacterial activity, with CPCD-3 inhibiting *E. coli* and *S. aureus* (15 mm and 12 mm zones) *via* membrane disruption and oxidative stress modulation, respectively. Biodegradation reached 94% in 100 days, and release studies showed sustained diffusion of NLCDs in food simulants. In prawn packaging trials, CPCD-3 preserved the pH (6.8–7.0), reduced the TVBN (28 mg/100 g), and maintained the microbial load (5 log CFU g<sup>-1</sup>) for over 15 days at 4 °C. These findings position NLCD-embedded CP films as next-generation, multifunctional active packaging materials with a clear mechanistic basis for their performance.

Received 4th July 2025  
Accepted 30th August 2025

DOI: 10.1039/d5fb00358j

rsc.li/susfoodtech

## Sustainability spotlight

The present study contributes significantly to the development of sustainable and biodegradable food packaging materials by utilizing neem leaf biomass to synthesize bioactive carbon dots (NLCDs) through a green hydrothermal process. These carbon dots were embedded into chitosan/PVA-based films using a solvent casting technique, significantly enhancing their antioxidant, antimicrobial, UV-blocking, and mechanical properties. The resulting films demonstrated excellent shelf-life extension when used for prawn packaging, maintaining freshness and reducing spoilage for up to 15 days under refrigerated conditions. By repurposing natural waste and eliminating synthetic additives, this work addresses both food preservation and environmental concerns, offering a promising solution for eco-friendly and active food packaging systems.

## 1 Introduction

Food packaging materials made of petroleum, synthetic, and non-biodegradable polymers continue to pose complex issues. These substances persist as environmental trash for a long period of time. Micro- and nano-plastics are released into the environment when they break down, endangering biodiversity.<sup>1</sup> These plastics are so ubiquitous that they contaminate the soil, water, and air, affecting habitats on land as well as in the ocean. Food safety is a concern since plastic contaminants seep into

<sup>a</sup>Department of Chemistry, Karnatak Science College, Dharwad 580001, Karnataka, India. E-mail: dr.saraswatomasti@yahoo.com<sup>b</sup>Indian Institute of Packaging, Bengaluru, 562132, Karnataka, India<sup>c</sup>Sustainable Energy & Nanomaterials Technology Research Applications Lab, Atria Institute of Technology, Bengaluru 560024, Affiliated to Visvesvaraya Technological University, Belagavi, Karnataka, India<sup>d</sup>Drosophila and Nanoscience Research Laboratory, Department of Applied Genetics, Karnatak University, Dharwad 580003, India<sup>e</sup>Department of Chemistry, Karnatak University, Dharwad 580003, Karnataka, India

food and water sources.<sup>2</sup> Furthermore, consumption of microplastics may harm one's health, which is why studies on the effects of microplastics on the human health are still being conducted, although it is unclear to what extent;<sup>3</sup> meanwhile, food packaging has undergone a dramatic shift in the last few years due to the increased need for environmentally friendly, sustainable, and active packaging materials as awareness of food safety and environmental issues has grown globally.<sup>4,5</sup> One cutting-edge strategy in this field is the creation of functional films with enhanced qualities that can decrease food waste, increase the shelf life of perishable goods, and improve the overall health of consumers.<sup>6</sup> To head towards a sustainable packaging direction, various methods are employed for the quality preservation of food, *viz.*, coating,<sup>7</sup> chemical processing,<sup>8</sup> blanching,<sup>9</sup> exposure to ultraviolet irradiation,<sup>10</sup> plasma treatment,<sup>11</sup> packaging in a modified atmosphere,<sup>12</sup> intelligent packaging systems,<sup>13,14</sup> and active packaging films.<sup>15,16</sup> Active food packaging not only sustains against microbes but also extends the shelf life of the packed food. Active food packaging protects food from harmful UV rays, which may otherwise cause UV-mediated oxidation of food.<sup>17</sup> Furthermore, it controls the exchange of gases between the surrounding air and the packed product, thereby controlling the amount of respiration and prolonging the ripening and spoiling stages.<sup>17</sup> Using an active food packaging material with antimicrobial properties is crucial because most foodborne illnesses result from microbial harm during storage and may cause the loss of food essence.<sup>18,19</sup>

In recent times, scientists have developed active packaging films that crucially contribute to food preservation by utilizing a variety of nanomaterials from diverse sources. Carbon dots (CDs), a novel class of nanomaterials, have lately been used as an abundant and affordable functional material in various fields.<sup>20</sup> These are spherical, zero-dimensional nanomaterials made of carbon, usually smaller than 20 nm.<sup>21</sup> Unlike other carbon-based nanomaterials, these CDs exhibit distinct photoluminescent features because of their small size.<sup>22</sup> They also show additional advantageous characteristics like low toxicity, biocompatibility, water solubility, and photoluminescence.<sup>23</sup> Their tunable surface functional groups and size also result in excellent adsorption interactions with biological surfaces.<sup>24</sup> CDs exhibit a sophisticated chemical composition comprising a carbon-rich core and a distinct surface functional group.<sup>25</sup> The foundational structure of these CDs varies based on the synthesis technique employed and the specific carbon source utilized in their creation. On the other hand, the functional groups are directly derived from the source. CDs typically comprise carboxyl, amino, hydroxyl, and various other groups that govern their surface properties.<sup>26</sup> Apart from their relevance in biological applications, recent studies have highlighted the robust antioxidant potential<sup>27</sup> and moderate antimicrobial<sup>28</sup> attributes associated with CDs. According to the literature survey and recent reports on the cytotoxicity of CDs, which are synthesized from biogenic sources such as plant and animal-based, they exhibit a remarkably low or negligible level of cytotoxicity.<sup>29,30</sup> Swarup Roy *et al.* conducted a study on the cytotoxicity of enoki mushrooms, which showed negligible to no toxicity even at high concentrations. Additionally, numerous

investigations have demonstrated that CDs, whether or not their surface is modified, exhibit extremely low toxicity. Further studies conducted on CDs exhibited quantities ranging from 0.01 to 0.1 g L<sup>-1</sup>, resulting in a negligible loss (around 10–15%) of healthy cells. Hence, CDs could be employed in applications like food packaging and cell labelling.<sup>17</sup> These food-grade CDs, devoid of harmful and non-food-grade chemicals in their synthesis, are considered highly bio-compatible and pose minimal to zero toxicity concerns in the context of food packaging applications. Their origin from natural and edible sources enhances their safety profile, making them an environmentally sustainable and health-conscious choice for use in food packaging materials. These specific properties render them appealing materials for the exploration of novel applications, particularly in packaging.

For the development of active packaging films, bio-based polymers, such as polysaccharides, proteins, and polyacids, surpass synthetic petroleum-derived polymers in terms of safety, biodegradability, biocompatibility, environmental friendliness, and sustainability.<sup>31</sup> Hence, there is a growing preference for their utilization. There is a burgeoning interest in formulating binary composite films by amalgamating polysaccharides and synthetic biodegradable polymers to create functional packaging films based on biopolymers.<sup>32</sup> This endeavour aims to harness the inherent strengths of each constituent while mitigating their individual limitations. It is anticipated that such a hybrid film would leverage the benefits of each component while offsetting its drawbacks.

Chitosan (CS) exhibits tremendous potential for food packaging and in various other fields because of its barrier properties and excellent film-forming ability.<sup>33–36</sup> However, its maximum functioning is restricted by inherent limitations, such as poor mechanical properties, solubility, primarily in acidic conditions, and diminished antibacterial efficacy at pH levels over 6.5.<sup>37,38</sup> A strategic approach to overcoming these drawbacks involves blending CS with diverse polymers, such as gelatin,<sup>39</sup> polylactic acid (PLA),<sup>40</sup> and notably, polyvinyl alcohol (PVA).<sup>41</sup> Among synthetic polymers, PVA is particularly noteworthy due to its high biodegradability, nontoxic nature, and superior miscibility and film-forming properties.<sup>42–44</sup> Leveraging the compatibility between PVA and CS, hydrogen bonding acts to immobilize CS with the PVA matrix. This integration augments the mechanical prowess of CS significantly.<sup>45</sup> The addition of PVA in varying quantities significantly improves the overall performance of the composite films. It fosters plasticization, elevates elasticity, augments elongation, bolsters tensile strength, and fortifies water and oxygen barrier properties.<sup>46,47</sup> Because of the collaborative synergy between CS and PVA, the limitations of CS are mitigated, and the resulting blend is positioned as a flexible and effective antibacterial agent in the realm of food packaging materials.<sup>48</sup> According to previous research, a composite film with superior physical properties was obtained by mixing chitosan and PVA (3 : 1). Furthermore, the amalgamation of a bioactive and eco-friendly filler, specifically CDs, serves to augment the functional attributes of the blended film. This optimum film has the scope to be used as an active packaging material. Notably, there is a discernible dearth of



reports documenting the utilization of NLCDs in the fabrication of CS/PVA-based functional composite films for food packaging applications.

Recent research has advanced the design of sustainable and multifunctional food packaging systems, including greener polymers,<sup>49</sup> natural biomass-based films with improved biodegradability and antimicrobial properties,<sup>50–52</sup> and smart nano systems with integrated sensing functions.<sup>53</sup> These studies collectively emphasize the urgent need for packaging that not only extends shelf life but also minimizes environmental impact. Building on this progress, the present work introduces a green nanotechnology-based strategy that employs phytochemically rich neem leaves to synthesize fluorescent and bioactive carbon dots (NLCDs), which are subsequently integrated into a CP matrix. This approach leverages the dual role of NLCDs as mechanical reinforcers and active agents with antioxidant, antibacterial, and UV-shielding properties, thereby addressing the critical gap of simultaneously achieving structural enhancement, multifunctional bioactivity, and high biodegradability in a single, sustainable packaging platform. This work bridges fundamental research and scalable production, aligning with the principles of the circular economy.

To the best of our knowledge, this study presents a novel combination of NLCDs embedded in chitosan-based films, which have not been explored yet, specifically tailored for sustainable prawn packaging applications, addressing the dual challenge of enhancing food preservation while promoting eco-friendly packaging solutions. Thus, the main aim of this research was to create multifunctional films by adding NLCDs to a CS/PVA composite matrix and evaluate the functional qualities of the prepared films. It was hypothesized that adding NLCDs would greatly enhance the mechanical strength, barrier properties, antibacterial activity and antioxidant properties of CS/PVA films. Furthermore, it is anticipated that the structural

integrity and release kinetics of the implanted NLCDs within the matrix will display regulated and prolonged behaviour, increasing the potential for use in the food packaging industry (Fig. 1 and 2).

## 2 Materials and methods

### 2.1 Materials

A low molecular weight chitosan,  $1526.464 \text{ g mol}^{-1}$ , with 5–20 mPa s, 0.5% in 0.5% acetic acid at 20 °C, was purchased from TCI. Polyvinyl alcohol (PVA), with a molecular weight of  $125\,000 \text{ g mol}^{-1}$ , 98–99% hydrolysis, was purchased from Thomas Baker Pvt. Ltd., Mumbai. Acetic acid, 2,2-diphenyl-1-picrylhydrazyl (DPPH), hydrogen peroxide ( $\text{H}_2\text{O}_2$ ), anhydrous  $\text{CaCl}_2$ , ethanol, magnesium oxide (MgO), hydrochloric acid (HCl) and all other chemicals were purchased from Merck Life Science Pvt. Ltd., Mumbai. The neem leaves (*Azadirachta indica*) were collected from the botanical garden area of Karnatak University, Dharwad, Karnataka, India. The prawns were purchased from the local market. All the polymer blends were prepared using double-distilled water.

### 2.2 Preparation of carbon dots

Carbon dots (CDs) were synthesized using a one-step, easy hydrothermal method using freshly harvested neem leaves. After being dried out in the shade, the neem leaves were milled into a fine powder. In a Teflon-lined stainless-steel reactor with a 100 mL capacity, 10 grams of this neem leaf powder were mixed with 100 mL of distilled water. The mixture was then heated for 4 hours at 150 °C. After heating, the resultant solid was separated using centrifugation for 20 minutes at 10 000 rpm. The resulting supernatant was filtered using a membrane filter, with a 25 mm diameter made of nylon material and a 0.2  $\mu\text{m}$  pore size, purchased from Merck. The

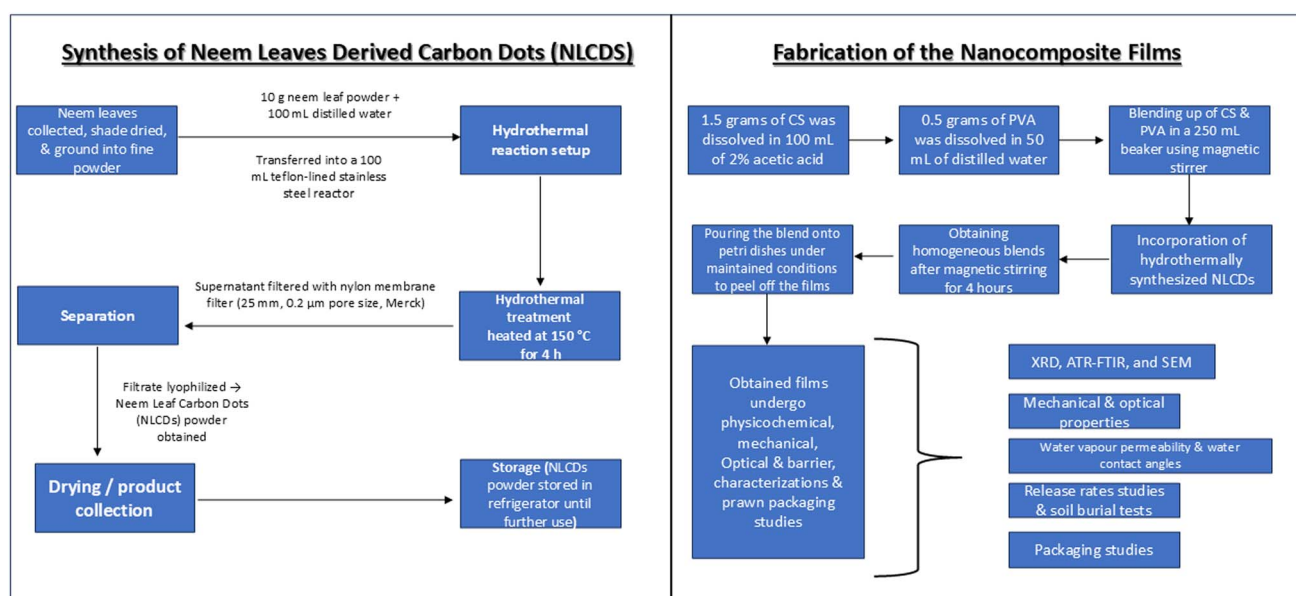


Fig. 1 Flow chart of the work.



## Reaction Mechanism of the Work

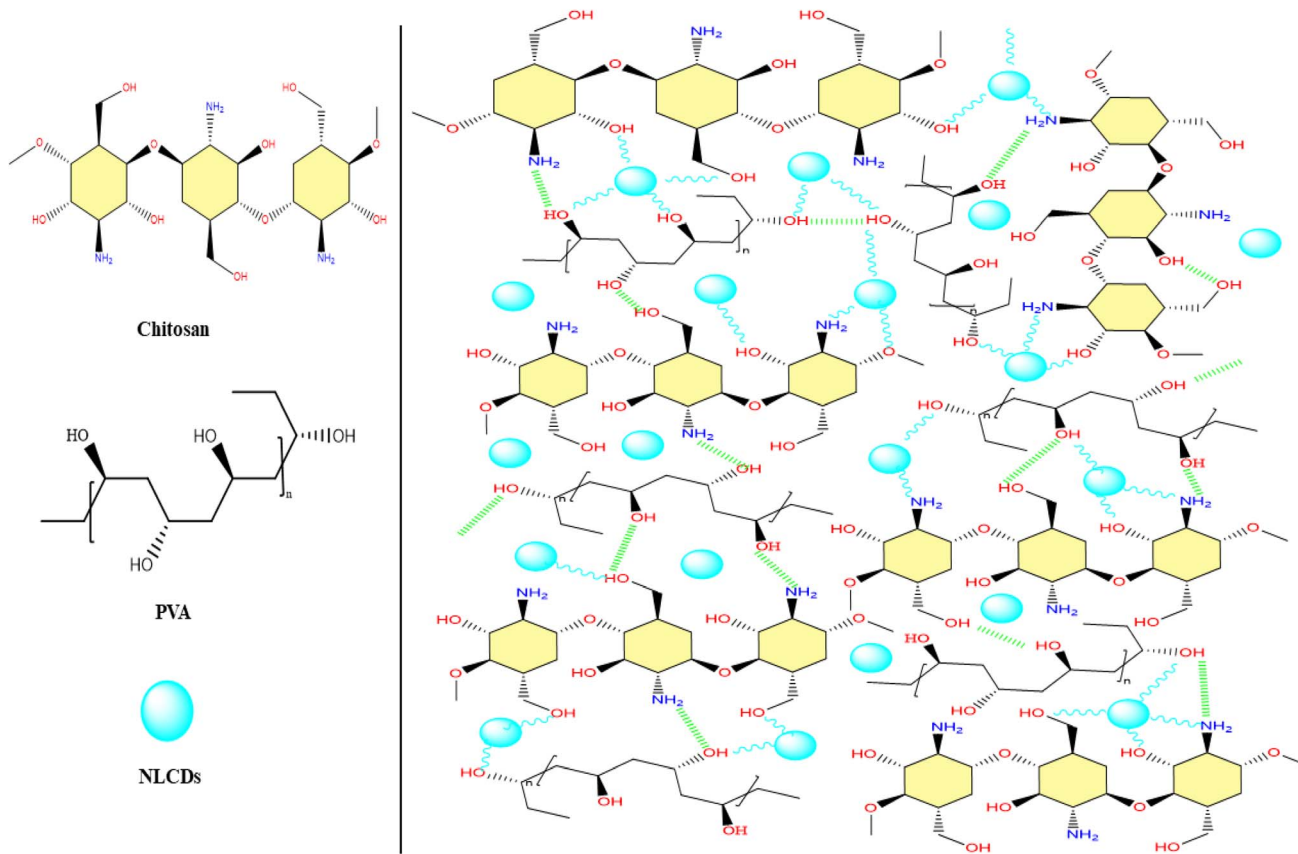


Fig. 2 Reaction mechanism of the work.

filtrate was then subjected to lyophilization to produce neem leaves carbon dots (NLCs) in powder form, which were kept in a refrigerator until the additional testing.<sup>54</sup> The quantum yield (QY) of the NLCs was determined using quinine sulfate in 0.1 M H<sub>2</sub>SO<sub>4</sub> (QY = 0.54) as a standard, yielding a QY of 0.21(21%) for the synthesized NLCs.

### 2.3 Fabrication of nanocomposite films

The films using a blend of chitosan (CS) and polyvinyl alcohol (PVA) were developed through a solvent casting technique. Initially, 1.5 grams of CS was dissolved in 100 mL of 2% acetic acid and stirred for an hour, while 0.5 grams of PVA was dissolved in 50 mL of double-distilled water, stirred at 70 °C for 30 minutes. The solutions were combined and mixed for 30 minutes in a 500 mL beaker. Later, 0.2 mL of glycerol was added to the solution and stirred for 3 hours. NLCs (1%, 3%, and 5%, based on the weight of the polymeric solid content) were incorporated and stirred for an additional hour. The blended solutions were cast onto glass Petri dishes and air-dried for seven days at room temperature. After drying, the films were gently removed from the glass Petri dishes and conditioned at 25 °C and 50% relative humidity for at least 72 hours. Control films, solely composed of CS/PVA without NLCs, were prepared for comparison. These films were labelled as CP (control film), CPCD-1 (1% NLCs), CPCD-2 (3% NLCs), and

CPCD-3 (5% NLCs), reflecting variations in the NLCs content. The characterization of the resulting films was conducted using the following established procedures.

### 2.4 Characterizations of NLCs and fabricated nanocomposite films

**2.4.1 Characterization of NLCs.** UV-vis spectrophotometer (JASCO V-670, Japan) and fluorescence spectrophotometer (F-7000, Japan) were used for the study of optical properties. TEM-EDS (JEOL JEM 2100 Plus, Japan) was used to analyze the morphology and elemental mapping, while ATR-FTIR (Thermo Nicolet, USA) was used to examine the chemical structures. XRD (Rigaku D/Max-IIA, Japan) was used to determine the interlayer spacing and antioxidant activity was evaluated *via* the DPPH and H<sub>2</sub>O<sub>2</sub> scavenging assays.<sup>55–57</sup>

**2.4.2 Nanocomposite film characterizations.** SEM (JSM-IT500, Japan) was used for morphology; ATR-FTIR and UV-vis spectrophotometry were used to analyze the structural and optical properties, while XRD was used to assess the crystallinity.<sup>58</sup> Mechanical properties, including tensile strength, elongation, and elastic modulus, were evaluated using UTM (DAK, India). Water vapour permeability (WVP) and water contact angle (WCA) were measured using standard methods.

**2.4.3 Functional studies.** The release kinetics of NLCs in food simulants were monitored using UV-vis spectroscopy.<sup>54,59</sup>



The antioxidant activity of the films was tested *via* DPPH and H<sub>2</sub>O<sub>2</sub> assays. The antibacterial properties were assessed using agar well diffusion against *E. coli* and *S. aureus*. Their biodegradability was evaluated *via* a soil burial test.

**2.4.4 Prawn packaging assessment.** Prawns were stored in CP and CPCD-3 films for 15 days at 4 °C. The tests included pH, Total Volatile Basic Nitrogen (TVB-N) using a Micro Kjeldahl equipment, Total Viable Count (TVC) by plate count agar, and qualitative assessments of firmness and odour.

The detailed characterization procedures, including the equations, are provided in the SI.

## 3 Results and discussion

### 3.1 Characterizations of NLCDs

The synthesized NLCDs solution is yellowish brown in hue, but the quantum confinement effect causes it to transform to dark green when exposed to ultraviolet light<sup>60,61</sup> (Fig. 3). The identified phenomenon aligns with findings from prior research on carbon dots synthesized using enoki mushrooms.<sup>17</sup> UV-vis absorption spectra were utilized to track the optical characteristics of water-soluble NLCDs.

A distinct peak at approximately 220 nm and around 270 nm indicated the  $n-\pi^*$  and  $\pi-\pi^*$  transitions of either C=O or C-OH and C=C bonds,<sup>62</sup> affirming the successful production of carbon dots *via* the carbonization process of neem leaves (Fig. 3(A)). The photoluminescence spectra of the NLCD solution exhibited a robust emission peak in the blue light

spectrum, roughly at 450 nm. Notably, the emission light could be tuned between 300 and 480 nm by varying the incident excitation wavelength, as depicted in Fig. 3(B). As the excitation energy increased within this range, a noticeable red shift occurred in the emission peak, albeit with reduced intensity. Surface defects are considered the probable cause behind this coordinated emission, generating diverse energy states and hence, tunable emissions.<sup>63</sup> TEM analysis confirmed that the NLCDs were uniformly dispersed, nearly spherical, and ~8 nm in size. This uniform distribution enhances surface interactions with analytes, thereby improving fluorescence sensitivity and stability in food packaging applications.<sup>64</sup> These findings closely resemble those of previously published research on neem leaf-mediated carbon dots.<sup>65</sup> The quantum yield (QY) of the NLCDs was determined using quinine sulfate in 0.1 M H<sub>2</sub>SO<sub>4</sub> (QY = 0.54) as a standard, yielding a QY of 0.21(21%) for the synthesized NLCDs.

### 3.2 Antioxidant properties of NLCDs

DPPH and H<sub>2</sub>O<sub>2</sub> radical scavenging assays were used to evaluate the antioxidant characteristics of NLCDs at different doses (12.5, 25, 50, and 100 µg mL<sup>-1</sup>). The DPPH experiment demonstrated the powerful antioxidant potential of NLCDs by showing an increase in their free radical scavenging activity as the concentration increased with the maximum activity recorded at 100 µg mL<sup>-1</sup>, as depicted in Fig. 4. Similarly, the H<sub>2</sub>O<sub>2</sub> scavenging assay demonstrated a significant decrease in

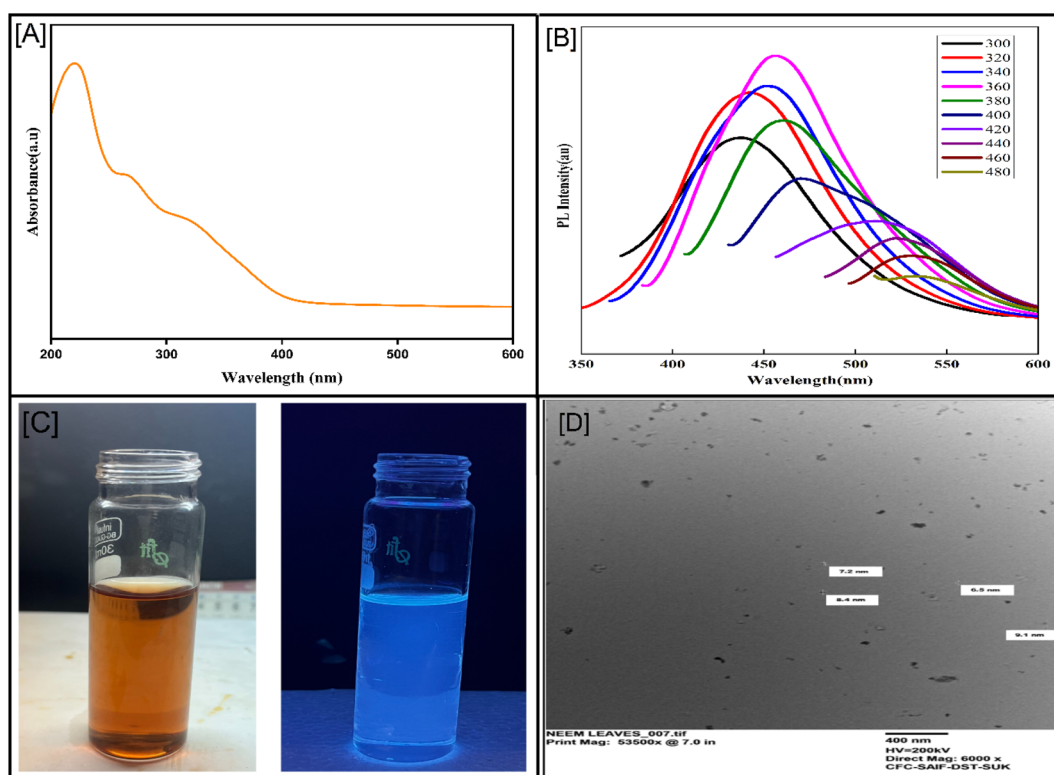


Fig. 3 (A) UV absorbance spectra, (B) photoluminescence spectra, (C) visualisation under visible and UV light, and (D) TEM image of neem leaf-derived carbon dots (NLCDs).



absorbance at 230 nm as NLCDs concentration increased, demonstrating their efficacious capacity to scavenge  $\text{H}_2\text{O}_2$  radicals. The concentration of  $100 \mu\text{g mL}^{-1}$  was found to have the maximum scavenging activity of 85%. The median inhibitory concentration ( $\text{IC}_{50}$ ) was calculated to be 18 and  $40 \mu\text{g mL}^{-1}$  for DPPH and  $\text{H}_2\text{O}_2$  scavenging, respectively. This data is in accordance with the DPPH scavenging power of carbon dots derived from neem leaves, priorly synthesized by Gedda *et al.*, with an  $\text{IC}_{50}$  of  $13.87 \mu\text{g mL}^{-1}$ .<sup>66</sup>

These results imply that NLCDs have strong antioxidant properties, most likely because neem leaves have a number of active phytochemicals, such as azadirachtin, alkaloids, nimbolinin, nimbin, quercetin, triterpenes and others, which are known for their radical scavenging and antioxidant properties.<sup>67</sup> The presence of  $-\text{OH}$  and  $-\text{COOH}$  groups on the surface of NLCDs can be attributed to radical scavenging by donating

hydrogen atoms, with stabilization occurring through bond reconfiguration or electron delocalization within the aromatic core.<sup>56</sup> This demonstrates their potential use as organic antioxidants in a variety of industries, such as biomedicine and food preservation.

### 3.3 FTIR spectra of NLCDs

Insights into the chemical structure and functional groups of NLCDs can be gained by interpreting the FTIR peaks, as shown in Fig. 5(A). Among the notable peaks found, the peak at about  $3400 \text{ cm}^{-1}$  is associated with the stretching vibration of hydroxyl ( $-\text{OH}$ ) groups, suggesting that the NLCDs surface contains alcoholic or phenolic functional groups. The stretching vibrations of the C–H bonds are responsible for another notable peak at around  $2900 \text{ cm}^{-1}$ , which implies the presence of methyl groups or aliphatic hydrocarbons. C=C stretching vibrations are indicated by peaks in the  $1600\text{--}1700 \text{ cm}^{-1}$  range, which would suggest the presence of aromatic C–C double bonds. Moreover, the peaks observed between  $1400$  and  $1500 \text{ cm}^{-1}$  can be associated with methyl or methylene group C–H bending vibrations. Peaks found between  $1700$  and  $1750 \text{ cm}^{-1}$  can be used to infer the presence of carbonyl ( $\text{C}=\text{O}$ ) groups. Furthermore, the peaks in the  $1000\text{--}1200 \text{ cm}^{-1}$  range could be associated with C–O stretching vibrations, indicating the presence of carboxylic acids, ethers, or alcohols.<sup>68</sup>

### 3.4 XRD diffractograms of NLCD

For understanding further about the nanostructure of prepared materials, XRD is beneficial. The broad peak (002 planes) centred at  $2\theta = 21.87$  in the XRD pattern of NLCDs, as shown in Fig. 5(B), corresponds to an interlayer spacing distance ( $d_{hkl}$ ) of  $2.085 \text{ \AA}$ , which is less than the lattice spacing in graphite ( $3.34$

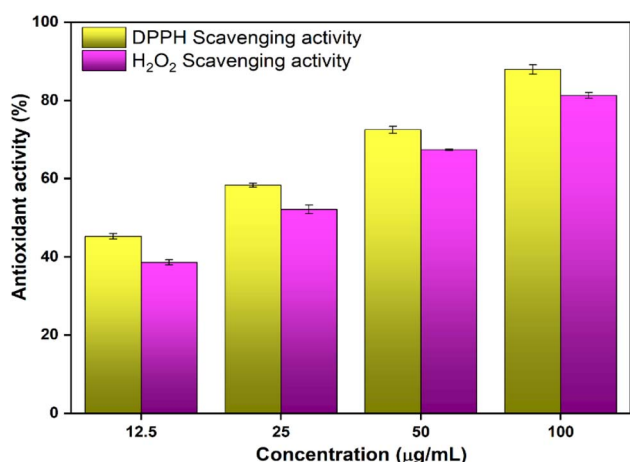


Fig. 4 Antioxidant activity of NLCDs at different concentrations.

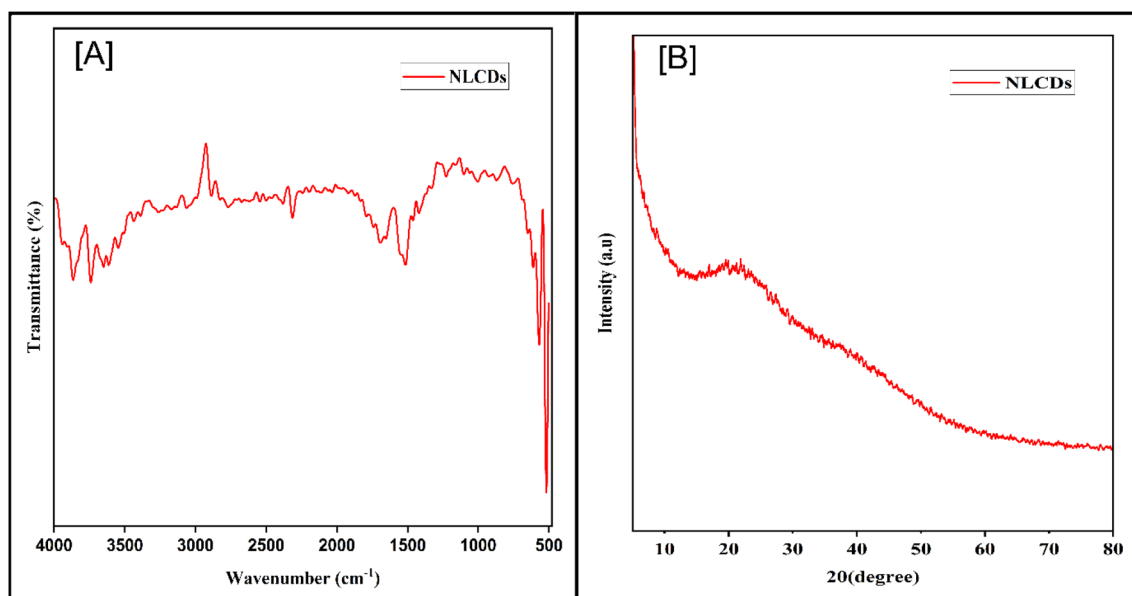


Fig. 5 (A) FTIR spectra and (B) XRD diffractograms of NLCDs.



Å). This demonstrates the presence of highly disordered graphitic-like carbon in the NLCDs nanostructure.<sup>68</sup>

### 3.5 Characterization of films

**3.5.1 Optical properties of films.** Blocking of light is crucial for packaging materials, as light predominantly causes food to decompose and oxidize by destroying the nutrients and physiologically active compounds. This leads to browning, rancidity, off-flavour, and the development of harmful toxins. One of the most important characteristics of food packaging films is their light transmittance, which denotes transparency and UV protection. The films were scanned at wavelengths between 200 and 700 nm. Light transmittance at 660 nm ( $T_{660}$ ) and 280 nm ( $T_{280}$ ) was measured to assess the transparency and UV barrier characteristics of the films (Fig. 6).<sup>69</sup>

The transmittance values (%) of nanocomposite films at wavelengths of 280 nm (UV region) and 660 nm (visible light) are displayed in Table 1. Additionally, it provides the UV-blocking potential of fabricated films in the UV-A and UV-B regions. The transmittance at 660 nm is fairly stable across all films, with a range of  $22.083\% \pm 0.51\%$  to  $21.964\% \pm 0.34\%$ . However, a noticeable drop in transmittance at 280 nm in the UV region is noted as the concentration of NLCDs increases from CPCD-1 to CPCD-3. For instance, CPCD-1 has

a transmittance of  $14.022\% \pm 0.40\%$  at 280 nm, whereas CPCD-3 shows a much lower transmittance of  $7.467\% \pm 0.17\%$  at the same wavelength, suggesting that higher NLCD concentrations considerably attenuate UV light. Additionally, the UV blocking capacity of the fabricated films in the UV-B region dramatically rose from  $64.833\% \pm 0.57\%$  in CP to  $99.634\% \pm 0.43\%$  in CPCD-3, demonstrating a much-improved UV-B blocking capability of films with higher NLCD concentrations.<sup>70</sup> A similar trend was also observed for the UV-A region. The high UV absorbance capacity of NLCDs in the film is responsible for its efficiency in blocking UV radiation. These results highlight the potential of NLCD-integrated films, especially CPCD-3, as efficient UV-blocking materials in food packaging applications that require vital protection against dangerous UV radiation, as UV rays cause food to oxidize and decay.<sup>71</sup>

### 3.5.2 Mechanical properties of the nanocomposite films.

The study systematically documented the mechanical properties of the active films. The addition of NLCDs resulted in a moderate increase in film thickness due to increased solid content. The pristine CS/PVA film showed a tensile strength (TS) of  $26.34 \pm 0.11$  MPa, which is consistent with previous findings for films based on CS/PVA. The strength of the film is due to the strong intermolecular interactions between PVA and the CS matrix. The interaction between the positively charged amino

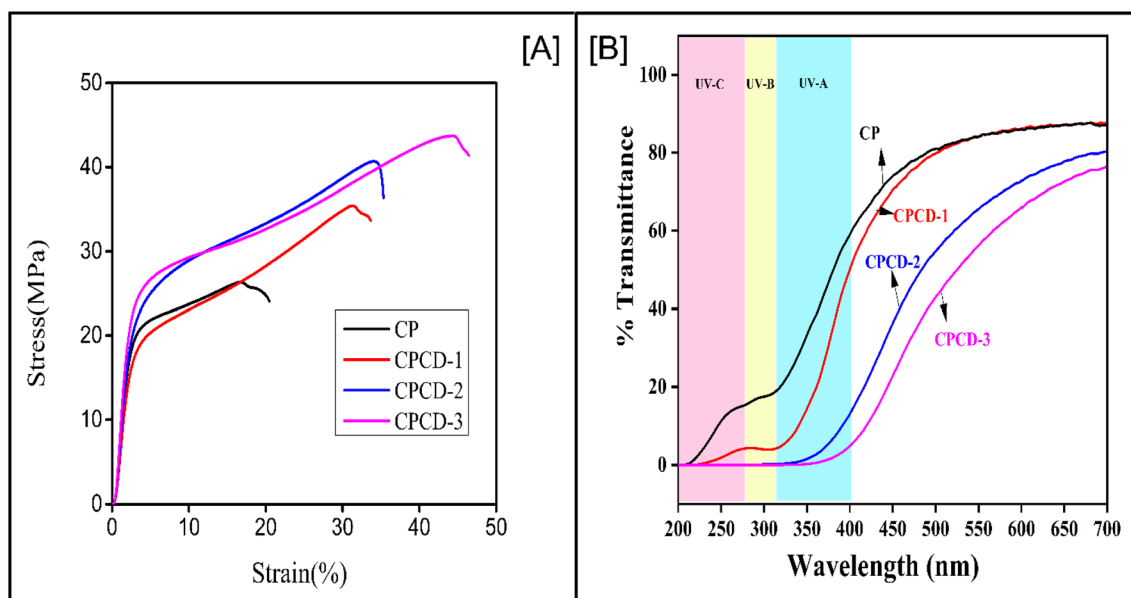


Fig. 6 (A) Stress–strain curves and (B) % transmittance graph under UV-A, UV-B, and UV-C regions of CP and CPCD films.

Table 1 Transmittance values (%) at 280 nm and 660 nm, and the UV blocking capacity in the UV-A and UV-B regions of CPCD films<sup>a</sup>

Films	% $T_{660}$	% $T_{280}$	% UV-A	% UV-B
CP	$22.083 \pm 0.51^a$	$24.174 \pm 0.28^b$	$61.127 \pm 0.57^a$	$64.833 \pm 0.57^a$
CPCD-1	$22.829 \pm 0.40^a$	$14.022 \pm 0.40^a$	$77.203 \pm 0.46^b$	$91.553 \pm 0.46^b$
CPCD-2	$22.283 \pm 0.46^a$	$13.58 \pm 0.34^a$	$95.895 \pm 0.43^c$	$99.689 \pm 0.50^c$
CPCD-3	$21.964 \pm 0.34^a$	$7.467 \pm 0.17^c$	$98.812 \pm 0.51^d$	$99.634 \pm 0.43^d$

<sup>a</sup> a–d denotes significant differences ( $n = 3, p < 0.05$ ).



Table 2 Thickness, mechanical properties, and water vapour permeability of CPCD films<sup>a</sup>

Films	Thickness (mm)	TS (MPa)	EB (%)	EM (GPa)	WVP × 10 <sup>-3</sup> (g m <sup>-1</sup> h <sup>-1</sup> Pa <sup>-1</sup> )
CP	0.07 ± 0.002 <sup>b</sup>	26.34 ± 0.11 <sup>b</sup>	20.476 ± 0.17 <sup>b</sup>	8.51 ± 0.040 <sup>b</sup>	1.54 ± 0.017 <sup>b</sup>
CPCD-1	0.08 ± 0.003 <sup>a</sup>	35.432 ± 0.34 <sup>c</sup>	33.696 ± 0.28 <sup>c</sup>	7.44 ± 0.046 <sup>c</sup>	1.94 ± 0.028 <sup>c</sup>
CPCD-2	0.09 ± 0.004 <sup>a</sup>	40.663 ± 0.23 <sup>d</sup>	35.357 ± 0.23 <sup>d</sup>	9.03 ± 0.051 <sup>d</sup>	2.5 ± 0.040 <sup>d</sup>
CPCD-3	0.1 ± 0.002 <sup>a</sup>	43.703 ± 0.46 <sup>a</sup>	46.448 ± 0.51 <sup>a</sup>	10.02 ± 0.057 <sup>a</sup>	3.08 ± 0.051 <sup>a</sup>

<sup>a</sup> a-d denote significant differences ( $n = 3, p < 0.05$ ).

groups and the -OH groups of CS with the -OH groups of PVA leads to physical interlocking and entanglement of the two materials, resulting in an increase in cohesion at the interface. This synergistic effect has an impact on the mechanical properties of the individual entities.<sup>72</sup> The addition of NLCDs significantly increased the TS because of the electrostatic interaction between the positively charged CS and the negatively charged NLCDs in the polymer matrix of PVA and CS (Table 2).

The incorporation of NLCDs into the CS/PVA matrix significantly impacted the elongation at break (EB) and elastic modulus (EM) of the resultant films. Specifically, the EB of CPCD-3 ( $46.448 \pm 0.51$ ) demonstrated a notable enhancement compared to the pristine CS/PVA film, while the EM showed a consistent increase with the addition of NLCDs. According to Swarup Roy *et al.*, the TS, EB, and EM of composites containing CDs are primarily influenced by the characteristics of the CDs employed, without following a specific trend.<sup>17</sup> For instance, in previous research by Xinyue Zhang *et al.*, chlorogenic acid CD-doped PVA films exhibited the TS and EB values of  $35.432 \pm 0.34$  MPa and 94.9%, respectively.<sup>73</sup> Similarly, the mechanical properties of CDs derived from enoki mushrooms in gelatin/carrageenan matrices displayed a proportional increase in TS and EB but a decrease in EM.<sup>17,73</sup> Likewise, another research finding indicates that the inclusion of a minimal proportion (0.5 wt%) of tea-derived cyclodextrin CDs in CS-based films

resulted in enhanced TS and a notable reduction in EB.<sup>74</sup> In the case of carboxymethyl cellulose (CMC) based films, the addition of CDs derived from citric acid led to a significant improvement in TS, approximately 55% compared to pristine CMC films.<sup>75</sup> Conversely, the incorporation of CDs synthesized from lactic acid bacteria into cellulose-based films reportedly decreased TS and substantially increased EB; hence, the impact of CDs on the mechanical properties of bio-based films can vary depending on the carbon source and the polymer type employed.

**3.5.3 FTIR and XRD studies of nanocomposite films.** The integration of NLCDs is indicated by significant spectrum variations in the ATR FTIR analysis of the CPCD series films (Fig. 7A). The spectrum of the CP reference film, characterized by the presence of solely CS and PVA, shows distinctive peaks of CS, including the amide I and II bands at  $1650 \text{ cm}^{-1}$  and  $1550 \text{ cm}^{-1}$ , respectively, and a broad O-H/N-H band spanning around  $3200\text{--}3400 \text{ cm}^{-1}$ .<sup>76</sup> The CPCD-1, CPCD-2, and CPCD-3 films show a significant shift and intensity change in these peaks upon the addition of NLCDs. In particular, as the NLCD concentrations increase in CPCD-1, CPCD-2, and CPCD-3, the C=O stretching vibration at  $1720 \text{ cm}^{-1}$  grows increasingly stronger, indicating that the NLCDs and polymer matrix are interacting. Furthermore, additional peaks corresponding to the vibrational modes of the functional groups on the surface of the NLCDs appear in the fingerprint area ( $1000\text{--}1500 \text{ cm}^{-1}$ ). These spectrum shifts indicate a growing degree of interaction

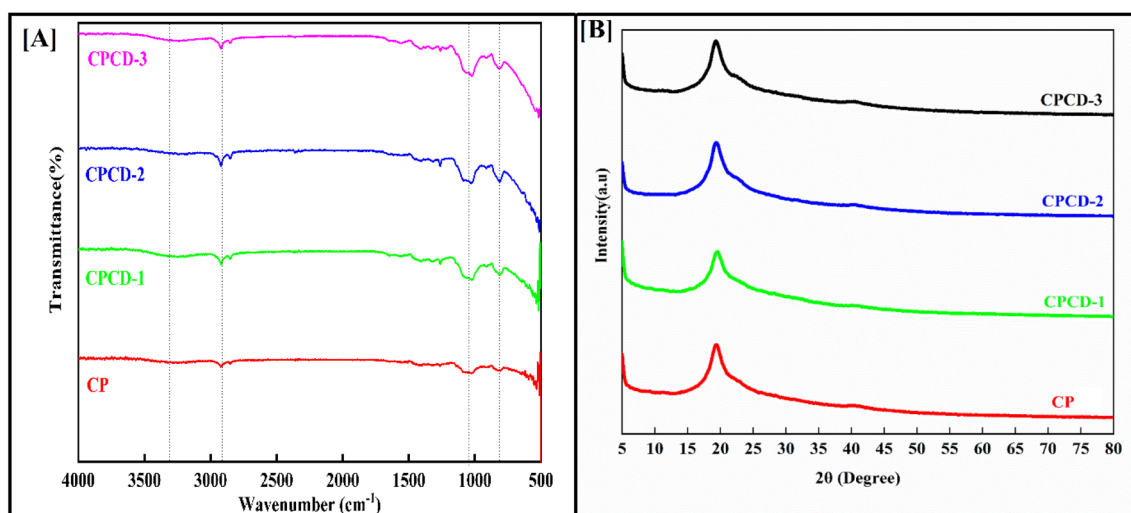


Fig. 7 (A) FTIR spectra and (B) X-ray diffractograms of CPCD films.



and integration with increased concentrations of NLCDs and validate the effective integration of NLCDs into the CP matrix.

The XRD study of the films in the CPCD series shows that the addition of NLCDs generates significant changes in the crystalline structure (Fig. 7B). The CP reference film, which primarily consists of CS and PVA, has distinctive broad diffraction peaks at approximately  $2\theta = 20^\circ$ , signifying the semi-crystalline composition of the CS/PVA blend. There is a noticeable variation in XRD patterns in the films comprising integrated NLCDs. The principal diffraction peak at  $2\theta = 20^\circ$  exhibits a progressive broadening and loss in intensity with increasing NLCD concentration, indicating a possible breakdown in the polymer crystalline structure. Furthermore, the creation of new crystalline phases or improved interaction between the NLCDs and the polymer matrix is indicated by the appearance of new peaks or shoulders at greater  $2\theta$  angles in CPCD-2 and CPCD-3. The effective integration of NLCDs into the CP films is confirmed by this disruption and restructuring of the crystalline structure, which is more noticeable at higher NLCD concentrations.<sup>77</sup>

**3.5.4 Morphology of nanocomposite films.** Scanning electron microscopy (SEM) was utilized to analyze the surface morphology of the fabricated films, revealing significant insights into their structural features (Fig. 8A–D). The pristine CP film exhibited a predominantly smooth and uncracked surface, with a few undissolved chitosan particles dispersed across the matrix, yet the overall integrity of the film remained uncompromised. As the concentration of NLCDs increased in CPCD-1, CPCD-2, and CPCD-3, the films maintained structural compatibility, with no visible phase separation, underscoring the effective dispersion of NLCDs at lower concentrations. However, CPCD-3 displayed a noticeable agglomeration of NLCDs, attributed to the hydrophilic nature of the particles, which tends to promote particle clustering at higher loadings.<sup>78</sup>

Despite the observed agglomeration, the CPCD-3 film retained a smooth and uncracked surface morphology, reflecting its robust structural integrity. This film also exhibited superior mechanical strength compared to its counterparts, indicating that the reinforcing effects of NLCDs outweighed the potential drawbacks of agglomeration.<sup>79</sup> These findings suggest that the incorporation of NLCDs into the CP matrix enhances its functional properties, with optimal performance observed at moderate concentrations.

**3.5.5 Water vapour permeability (WVP) and water contact angle (WCA).** The evaluation of water vapour permeability (WVP) of the prepared films is crucial to their use as food packaging materials. Water vapour transmission through open areas in the polymer matrix is measured by WVP. The WVP values for nanocomposite films are shown in Table 2. The neat film has a WVP of  $1.545 \times 10^{-3}$  ( $\text{g m}^{-1} \text{h}^{-1} \text{Pa}^{-1}$ ). The WVP of the CS/PVA matrix somewhat increased as the NLCD concentrations increased, according to the results (Table 2). The plausible explanation for this increase in WVP is that NLCDs are hydrophilic in nature, which means that when they are added to the CS/PVA polymer blend, initially rich in  $-\text{OH}$  groups, they increase the number of  $-\text{OH}$  groups. When compared to the pristine CP film, WVP was higher in NLCD-integrated films due to the facilitation of water molecule transport into the polymer matrix. Similar associations between the WVP and free  $-\text{OH}$  groups have also been observed in prior studies, such as that conducted by Jouki *et al.*, indicating a similar behaviour with the addition of hydrophilic extracts.<sup>80–82</sup> Moreover, the observed spike in WVP might have been caused by interactions between physisorbed water molecules and glycerol hydroxyl groups, facilitated simply by the greater plasticizer concentration in the NLCD-infused films.<sup>83</sup>

Water contact angle (WCA) measurements were used to evaluate the surface hydrophobicity of CS/PVA-based films

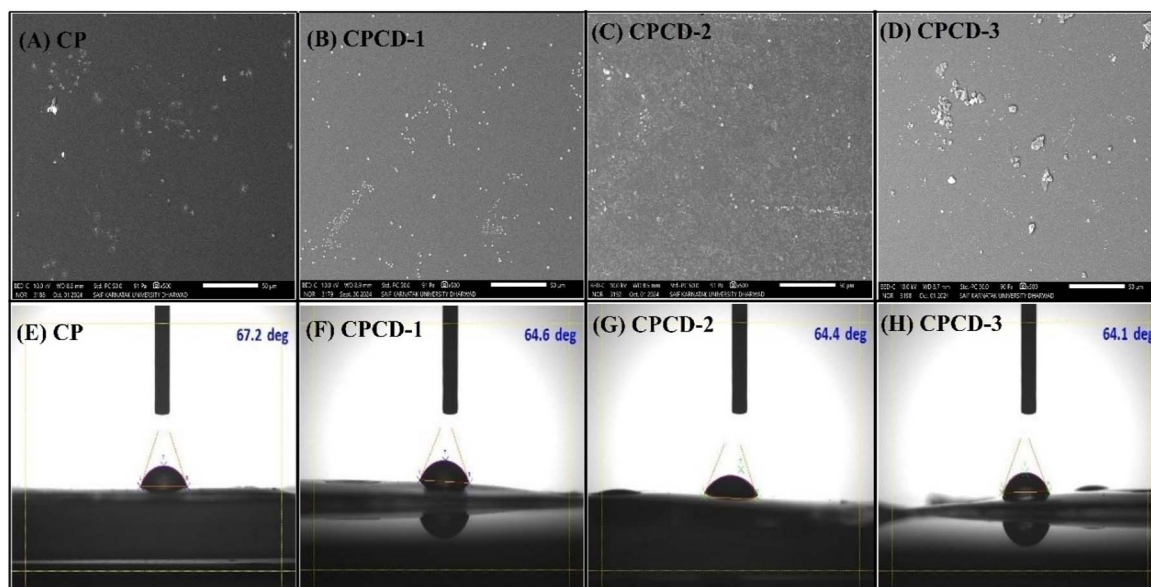


Fig. 8 (A–D) SEM images and (E–H) water contact angles of CP and CPCD films.



incorporating NLCDs. As the NLCD concentrations rise from 1 to 3 wt%, a decline in WCA is observed (Fig. 8E–H). More specifically, both prior to and following the loading of NLCDs, the WCA dropped from roughly 67.2° to 64.6°. WCA was marginally decreased by the addition of NLCDs, but there was no discernible variation in the values of the composite films on the inclusion of NLCDs. The WCA is used to determine the material roughness and surface functional groups. On the surfaces of CPCD-3 films, minor rough structures remained despite the increase in surface compactness brought about by the inclusion of NLCDs, suggesting the presence of free hydroxyl groups. The higher hydroxyl group concentration in CP films integrated with NLCDs was identified as the cause of the slight decrease in WCA, which indicates increased hydrophilicity. Furthermore, the increased hydrophilicity of NLCD-integrated CP films resulted from the hydrophilicity of the synthesized CDs. The surface hydrophilicity of composite films is primarily determined by the kind of nanofiller and polymer matrix that are employed; studies have shown that the incorporation of hydrophilic additives lowers the WCA of packaging films made of biopolymers.<sup>59,84</sup>

**3.5.6 Antioxidant activity of nanocomposite films.** The antioxidant activity of CP films infused with NLCDs was evaluated using DPPH and H<sub>2</sub>O<sub>2</sub> scavenging assays (Fig. 9A). The results demonstrated a significant improvement in scavenging capacity with increasing NLCD concentrations. The DPPH scavenging activities of CP, CPCD-1, CPCD-2 and CPCD-3 were 35%, 58%, 68%, and 82%, respectively. Similarly, the H<sub>2</sub>O<sub>2</sub> scavenging activity increased from 29% for CP to 47%, 62%, and 77% for CPCD-1, CPCD-2, and CPCD-3, respectively. The marked enhancement in antioxidant performance is attributed to the profound antioxidant properties of NLCDs. Incorporating NLCDs, rather than using the extract alone, significantly enhanced the antioxidant capabilities. This improvement is evident when compared to the study by Hameed *et al.*, where a chitosan-based polymeric matrix with 6% neem extract exhibited approximately 60% DPPH scavenging activity.<sup>85</sup> In contrast, the incorporation of just 5% NLCDs in the present study achieved a much higher scavenging activity of 82%. The

observed trend aligns with previous studies, where carbon quantum dots derived from natural sources exhibited enhanced antioxidant properties due to their ability to stabilize reactive oxygen species (ROS).<sup>86–88</sup> The incorporation of nanocarbon materials in chitosan-based matrices has similarly been reported to improve antioxidant performance by leveraging synergistic interactions between the polymer and nanoparticles.<sup>89</sup> In this study, the progressive increase in scavenging activity with higher NLCD concentrations underscores their role as effective radical quenchers, consistent with the findings in related biopolymeric systems.

**3.5.7 Antibacterial studies of nanocomposite films.** The antibacterial activity of various compositions of NLCDs was evaluated against *E. coli* and *S. aureus* using the agar well diffusion method (Fig. 9B). The results revealed that all active films exhibited clear zones of inhibition around the wells, indicating antibacterial activity. Among the samples tested, CPCD-3 showed the largest inhibition zones against both *E. coli* and *S. aureus*, with a zone of 15 mm against *E. coli* and 12 mm against *S. aureus*. This suggests that the 5% NLCDs concentration provided the most potent antibacterial effect, likely due to the higher availability of active antimicrobial species at this concentration. In contrast, CP showed minimal antibacterial activity, with inhibition zones of 5 mm for *E. coli* and 4 mm for *S. aureus*, attributed to the inherent antibacterial property of CS. CPCD-1 and CPCD-2 also displayed moderate antibacterial effects, with inhibition zones of 10 mm and 13 mm against *E. coli*, and 9 mm and 11 mm against *S. aureus*, respectively. These results indicate a dose-dependent increase in antibacterial activity with increasing concentrations of NLCDs. The observed antibacterial efficacy can be attributed to the unique properties of NLCDs, which are known to interact with bacterial cell membranes, leading to membrane disruption and subsequent bacterial cell death.

The antibacterial activity of CPCD films arises from the combined effects of CS cationic groups disrupting bacterial membranes and NLCDs modulating oxidative stress, with good polymer compatibility ensuring a uniform dispersion of active sites. Notably, antibacterial activity differs from broader

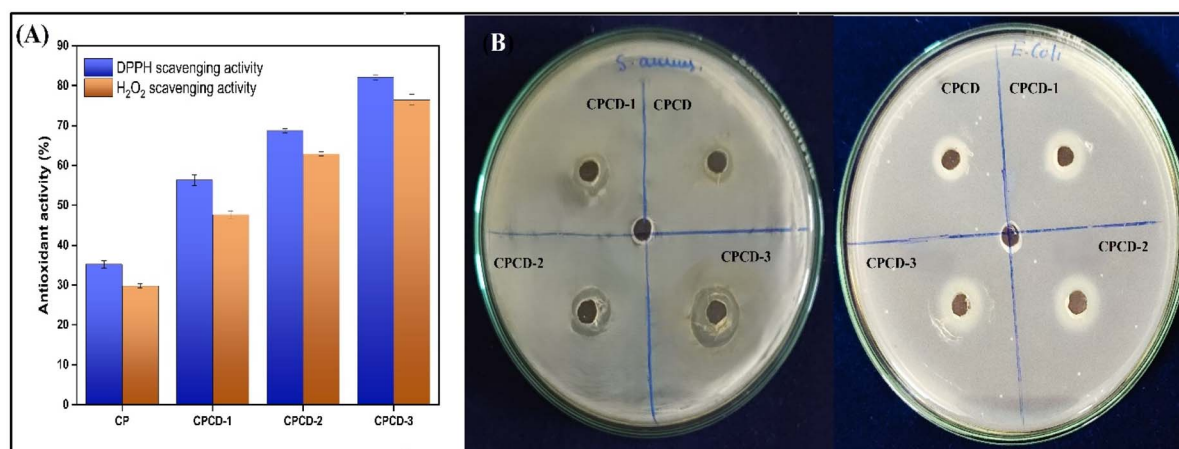


Fig. 9 (A) Antioxidant activities and (B) inhibition zones against *E. coli* and *S. aureus*.



antimicrobial effects that include other microorganisms, as highlighted in recent studies,<sup>90,91</sup> and our results against *E. coli* and *S. aureus* align with these reported mechanisms (Table 3).

**3.5.8 Degradation studies of nanocomposite films.** There are several substantial explanations for the enhanced biodegradability observed in NLCD-incorporated films used for food packaging materials (Fig. 10A). Firstly, NLCDs are naturally hydrophilic; they exhibit a susceptibility to hydrolysis in conditions that encourage degradation, like soil or compost, enabling the film structure to break down over time.<sup>94</sup> Furthermore, the addition of NLCDs boosts the breakdown process by integrating more active sites into the film matrix that are vulnerable to microbial attack.<sup>95</sup>

In addition, NLCDs may function as microbe colonization nucleation sites, which makes it easier for the enzymatic breakdown of organic materials in the film.<sup>96</sup> This phenomenon is further augmented by the amplified permeability of the film to water and microbial enzymes attainable in the presence of NLCDs. Also, the amalgamation of environmentally friendly polymers, such as CS and PVA, with NLCDs has a synergistic impact that enhances biodegradability, as these polymers are more susceptible to microbial degradation than conventional petroleum-based polymers.<sup>97,98</sup> The varying properties of the component materials can be the reason for the disparity in degradation rates exhibited in the tested films, which had percentages of 60%, 79%, 89%, and 94% degradation for CP, CPCD-1, CPCD-2, and CPCD-3, respectively. CS is resistant to deterioration in aqueous environments; therefore, the control film made of PVA/CS showed a relatively lower degradation rate than the films containing NLCDs. In contrast, the films containing NLCDs showed increased degradation, as the hydrophilic properties of NLCDs aid in their hydrolysis in soil conditions.

The FTIR analysis of fabricated films after 30 days of soil burial demonstrated clear evidence of biodegradation (Fig. 10B). A notable decrease in intensity was observed for peaks within the 2700–2900  $\text{cm}^{-1}$  range, associated with the C–H stretching of alkyl groups, indicating the breakdown of hydrocarbon chains. Similarly, the broad O–H stretching band at 3200–3400  $\text{cm}^{-1}$  showed reduced intensity, which could be attributed to diminished hydroxyl group interactions, likely due to microbial activity. Peaks in the 1200–1400  $\text{cm}^{-1}$  region, linked to C–N stretching and  $\text{CH}_2$  bending vibrations, also weakened, suggesting structural disruptions in amide linkages and the polymer backbone. Additionally, bands in the 700–900  $\text{cm}^{-1}$  range, corresponding to aromatic C–H out-of-plane bending, either disappeared or were significantly reduced, reflecting the degradation of aromatic structures.<sup>99,100</sup> This intricate interplay of factors underscores the potential of NLCD-containing films as promising candidates for sustainable food packaging materials, emphasizing their contribution to the broader objective of fostering environmental sustainability in packaging applications.

**3.5.9 Release rate studies.** Release kinetics in food packaging applications hinge largely upon the capacity of additives to permeate through packaging films. Extensive research has demonstrated that the swelling index, the water solubility of the

**Table 3** Comparison of the key findings of this work with those of previous relevant works

Sl. no.	Polymer base	Carbon dots (synthesised method)	Tensile strength (MPa)	Water vapour permeability	Inhibition zones		Reference
					<i>E. coli</i> mm	<i>S. aureus</i> mm	
1	Chitosan/PVA	Diammonium hydrogen citrate (hydrothermal method)	10.1	—	12	21	92
2	Chitosan/PVA	Ethylene diamine and citric acid: (microwave-assisted pyrolysis method)	57.74	0.260 ( $\text{g kPa}^{-1} \text{h}^{-1} \text{m}^{-2}$ )	—	—	93
3	Gelatin/carrageenan	Enoki mushrooms (hydrothermal method)	81.2	$1.02 \times 10^{-9}$ ( $\text{g m}^{-1} \text{h}^{-1} \text{Pa}^{-1}$ )	—	—	54
4	Chitosan/PVA (present work)	Neem leaves (hydrothermal method)	43.7	$3.8 \times 10^{-3}$ ( $\text{g m}^{-1} \text{h}^{-1} \text{Pa}^{-1}$ )	15	12	—



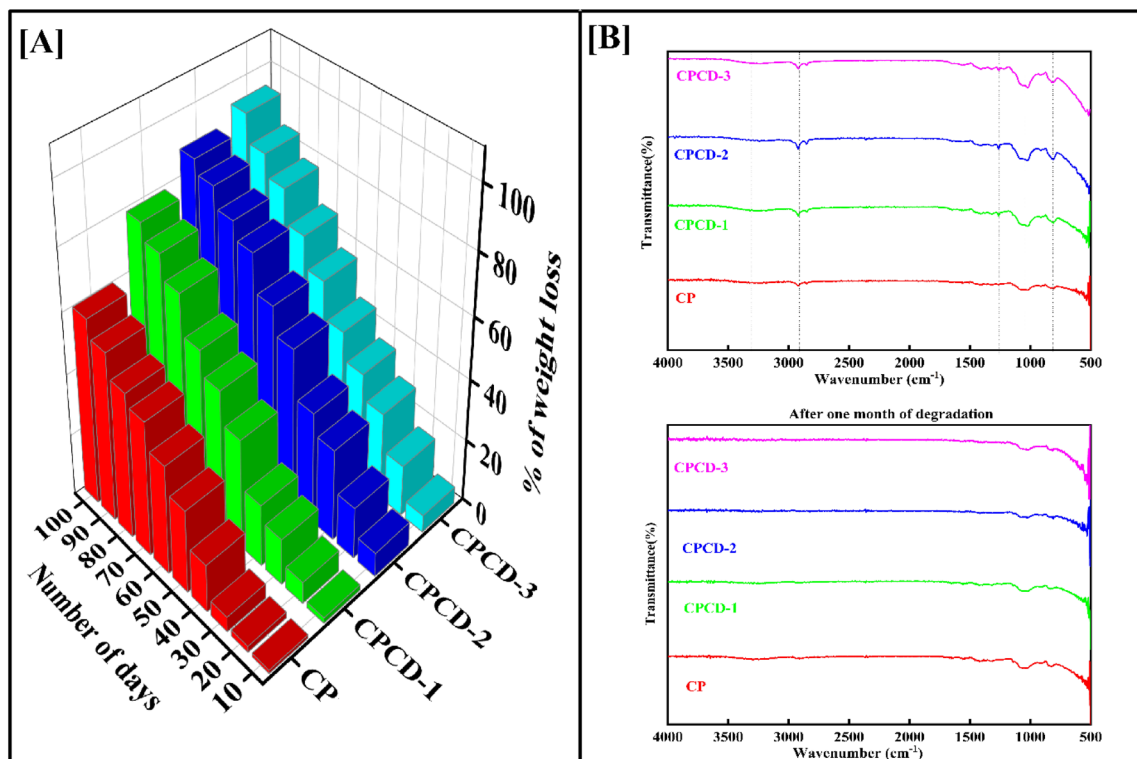


Fig. 10 (A) % of weight loss of soil-buried films and (B) FTIR spectra of films after 30 days.

polymer matrix, and the dispersion and solubility of nanoparticles in aqueous environments collectively influence the release of nanoparticles. Fig. 11A–C illustrates the release behaviors of various concentrations of nanostructured lipid carrier dispersions from CP matrices exposed to diverse food simulants. Notably, each profile exhibits a gradual release during the initial hour, likely attributable to the limited solubility of chitosan in water. Subsequently, the NLCD release reaches a plateau after 2 hours, with a deceleration observed in most instances. Interestingly, the release rate in alcohol solutions diminishes with increasing alcohol concentration, owing to the interaction of the solvent with NLCDs.<sup>54,101</sup>

Conversely, CP films containing 5% NLCDs in water and 10% ethanol exhibit the highest release rates, while those with 1% NLCDs in 50% and 95% ethanol show the lowest release rates. The cumulative release of NLCDs is notably higher in water and 10% ethanol compared to 50% and 95% ethanol, primarily due to the hydrophilicity and water solubility of NLCDs. Moreover, the release rate is contingent upon the solubility of the polymer matrix and the affinity of the solvent for NLCDs. Additionally, aqueous solutions facilitate rapid NLCDs release by promoting an open matrix structure. Conversely, alcohols exhibit limited interactions with CP polymers, resulting in a slower NLCDs release. This discrepancy underscores the influence of solvent type on release kinetics. Echoing the findings of Ezati *et al.* (2021), solvent affinity and polymer matrix solubility significantly impact the release rates, with water solutions yielding the highest recorded NLCDs release rates. Hence, the choice of simulant and NLCDs concentration in the polymer matrix crucially affects the release

behavior of NLCDs, suggesting potential enhancements in the functional properties of food contact films.<sup>54,101</sup>

### 3.6 Prawn packaging

**3.6.1 pH.** In a study comparing the efficacy of different packaging materials on the pH stability of refrigerated prawns, four groups were evaluated: unpacked prawns, prawns packed with a CS/PVA film, prawns packed with a CP film incorporating NLCDs, and prawns packed with commercial polythene (Fig. 11D). Over a typical storage period of 15 days at 4 °C, the unpacked prawns showed the most significant pH increase, indicating rapid spoilage and microbial activity. The initial pH of prawns (around 6.5–6.8) rose to 7.5 and higher in unpacked prawns due to bacterial production of basic compounds, such as ammonia. Prawns wrapped in a CP film exhibited better pH stability, with only a moderate increase to about 7.0, attributed to the antimicrobial properties of CS. The incorporation of NLCDs into the CP film further enhanced this effect, likely due to the additional antimicrobial activity of NLCDs, maintaining the pH closer to the initial value, around 6.8–7.0. The prawns packed in commercial polythene also showed a pH increase, but less pronounced than unpacked prawns, reaching around 7.2, as polythene provides a basic barrier but lacks antimicrobial properties. The results highlight the superior performance of CPC films, especially when enhanced with NLCDs, in preserving the quality and extending the shelf life of refrigerated prawns.<sup>102–104</sup>

**3.6.2 Total volatile basic nitrogen (TVB-N).** TVB-N refers to nitrogenous compounds, such as ammonia, trimethylamine,



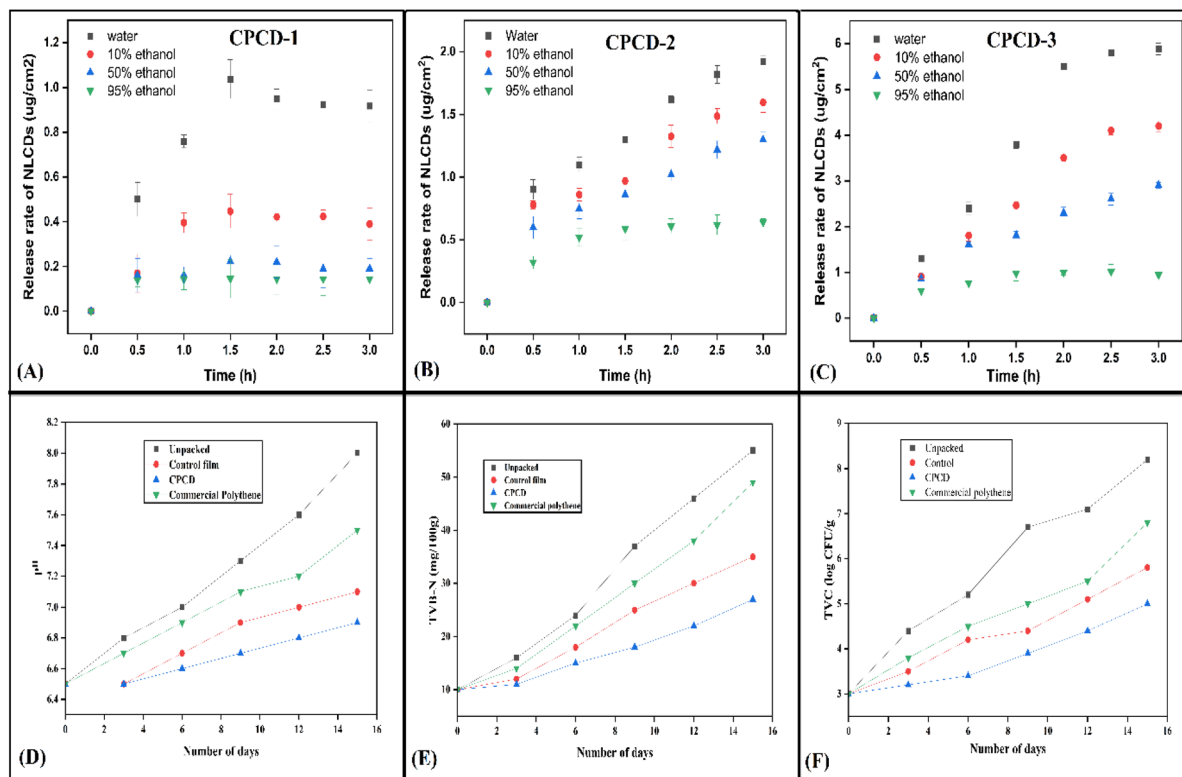


Fig. 11 Release rate of (A) CPCD-1, (B) CPCD-2, and (C) CPCD-3. Prawn packaging studies: effect of (D) pH, (E) TVB-N, and (F) TVC for different packaging materials.

and dimethylamine, produced during the degradation of proteins in meat and seafood. Its formation is influenced by microbial and enzymatic activity, with higher levels indicating spoilage.<sup>105</sup> In this study, the TVB-N levels of unpackaged prawn samples dramatically rose throughout the 15 day testing period, from 10 mg/100 g on day 1 to over 50 mg/100 g by the 15<sup>th</sup> day, indicating rapid deterioration (Fig. 11E). TVB-N levels in the prawn samples wrapped in CP films increased more slowly than normal, from 10 mg/100 g on the first day to 35 mg/100 g on the 15<sup>th</sup> day. Even greater preservation was achieved by the CPCD-3 film; by day 15, TVB-N levels had only increased to 28 mg/100 g. This implies that the CPCD-3 film successfully prevented the growth of volatile amines, most likely due to the antibacterial qualities of NLCs. A comparison of the commercial polythene packaging and the CPCD-3 film revealed that the latter's TVB-N levels increased more slowly, attaining 35 mg/100 g by day 12<sup>th</sup>. These findings show that CPCD-3 films are more effective in delaying spoilage, as indicated by the lower TVB-N levels during the storage period compared to the control film.<sup>106,107</sup>

**3.6.3 Total viable count (TVC).** TVC is yet another important metric to evaluate the proliferation of microorganisms in food products. Significant microbial proliferation was shown (Fig. 11F) by the TVC in unpackaged prawn samples, which increased from 3 log CFU g<sup>-1</sup> on day 3 to 8 log CFU g<sup>-1</sup> by day 15. The TVC increased more slowly in the prawn samples packed with CP films, going from 3 log CFU g<sup>-1</sup> on day 3 to 6 log CFU g<sup>-1</sup> by day 15. Further, a slower microbial growth was achieved by adding NLCs to the CP films (CPCD-3) within the

same time period, and the TVC levels increased from 3 log CFU g<sup>-1</sup> to just 5 log CFU g<sup>-1</sup>. The antibacterial qualities of NLCD, which successfully prevented bacterial development, are responsible for the decreased microbial growth. Comparable to the CP films, the commercial polythene packaging displayed a similar trend, although with somewhat higher TVC values, reaching 5.5 log CFU g<sup>-1</sup> by day 12. According to these results, CPCD-3 films offer better preservation than commercial polythene, which makes them a better choice for prolonging the shelf life of shrimp products. However, polythene does give some protection against microbiological growth.<sup>102,103</sup>

Overall, the data unequivocally show that the CPCD-3 film performs better than unpackaged and commercial polythene-packed samples in terms of maintaining prawn quality, as demonstrated by reduced TVB-N levels and TVC values. The inclusion of NLCs into a CP polymer matrix shows promise for improving food safety and increasing shelf life since it greatly reduces microbial growth and spoiling when added to packaging materials (Fig. 12).<sup>102,103,107</sup>

**3.6.4 Firmness and odour.** The firmness and odour were evaluated and listed in Table 4. It was found that CPCD-3 packaged prawns were fresh for 15 days when stored at 4 °C. The control film was better than the commercial polythene, preserving the prawn meat. This is attributed to the antibacterial properties of the CPCD-3 film, which ensures the growth of bacteria that eventually leads to meat spoilage.



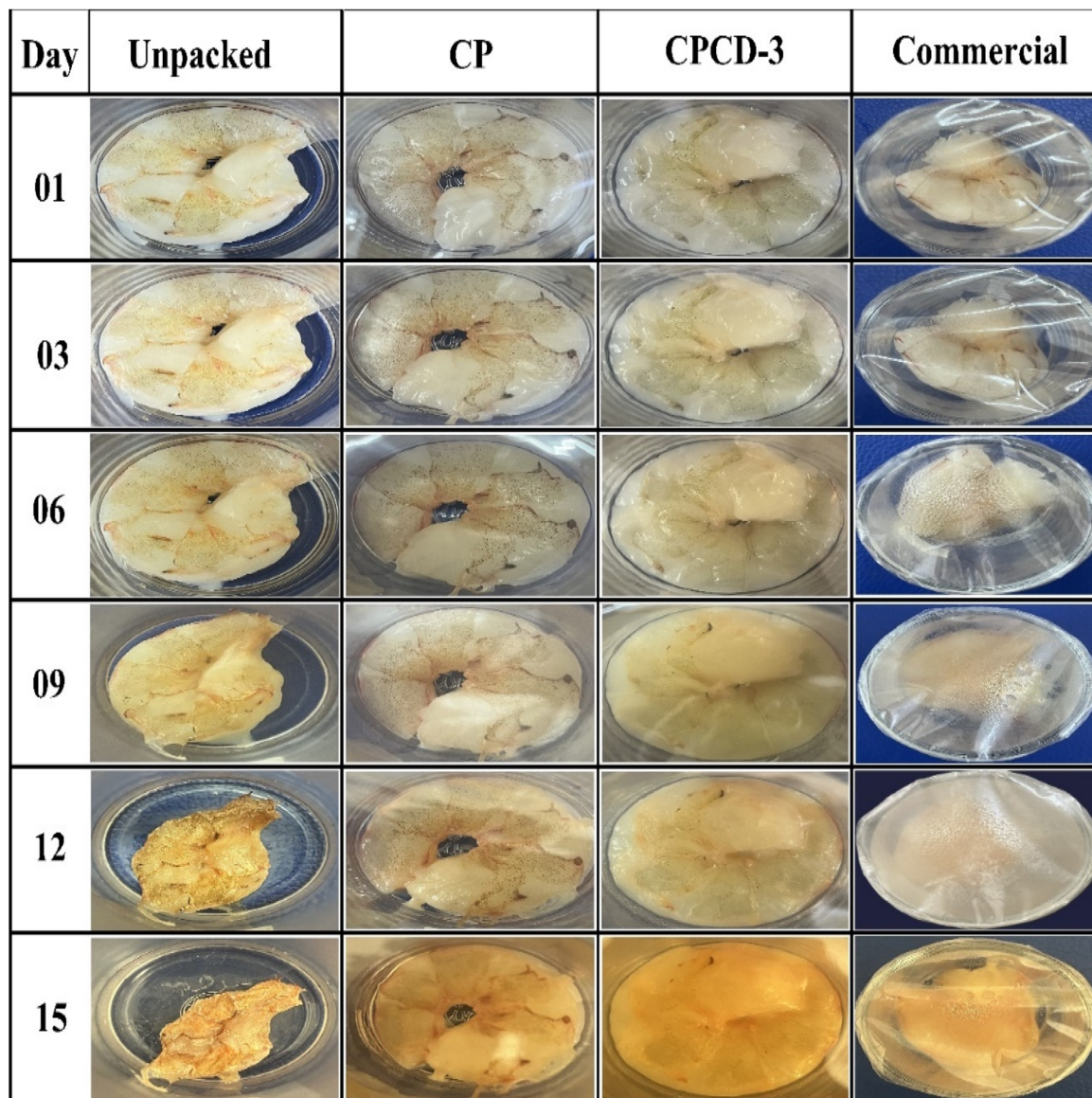


Fig. 12 Visual representation of unpacked and packed prawns for 15 days.

Table 4 Firmness and odour of packaged and unpackaged prawns kept at 4 °C

Samples	Test	Day						
		0	3	6	9	12	15	
Unpacked	Firmness	5 pt (firmness)/	4	3	2	1	1	
	Odour	fresh (odor)	Moderately off	Spoiled	Spoiled	Spoiled	Spoiled	
CP	Firmness		5	5	4	3	3	
	Odour		Fresh	Fresh	Fresh	Moderately off	Spoiled	
Polythene	Firmness		4	4	3	2	1	
	Odour		Moderately off	Moderately off	Spoiled	Spoiled	Spoiled	
CPCD-3	Firmness		5	5	5	4	4	
	Odour		Fresh	Fresh	Fresh	Fresh	Moderately off	



## 4 Conclusion

The study successfully achieved its objectives, demonstrating that the integration of NLCDs into the CS/PVA composite matrix substantially enhanced the functional properties of the films. This study differs from earlier reports by combining multiple functions, such as enhanced mechanics, UV-shielding, antioxidant and antibacterial activities, biocompatibility and rapid degradability within the NLCD-reinforced chitosan/PVA films, further validated in real food preservation trials. The resulting films exhibited remarkable improvements in antimicrobial and antioxidant activities, mechanical strength, UV barrier efficiency, and water permeability, validating the hypothesized benefits of NLCDs. Structural analysis confirmed the uniform incorporation of NLCDs without compromising the structural integrity of films, while release kinetics revealed a sustained and controlled release profile. Furthermore, CPCD-3 films demonstrated excellent biodegradability, addressing a critical limitation of conventional packaging materials. Packaging studies revealed that CPCD-3 films effectively extended the shelf life of prawns to 15 days under refrigeration at 4 °C. The CPCD films present a sustainable route by valorizing neem leaves through a low-energy, hydrothermal process, thereby reducing potential CO<sub>2</sub>/CH<sub>4</sub> emissions compared to conventional treatments.<sup>108–110</sup> Integration of biogenic chitosan with degradable PVA further minimizes reliance on fossil-based plastics. Overall, the approach suggests a markedly lower carbon footprint and potential carbon-negative profile under renewable energy and proper disposal pathways.<sup>111,112</sup> Despite these promising results, challenges remain in biodegradable packaging, including scaling up production, ensuring cost-effectiveness, and achieving optimal performance under diverse storage conditions. Nonetheless, these findings establish CPCD composite films as a sustainable and innovative solution for modern food packaging applications.

## Abbreviations

CS	Chitosan
PVA	Polyvinyl alcohol
CD	Carbon dots
NLCDs	Neem leaf-derived carbon dots
CP	Chitosan–PVA blend
CPCD	Chitosan/PVA/carbon dots
TEM-EDS	Transmission electron microscopy-energy-dispersive X-ray spectroscopy
UV-vis	Ultraviolet-visible spectroscopy
UTM	Universal testing machine
TS	Tensile strength
EB	Elongation at break
EM	Elastic modulus
FTIR	Fourier transform infrared spectroscopy
SEM	Scanning electron microscopy
XRD	X-ray diffraction
DPPH	2,2-Diphenyl-1-picrylhydrazyl
TPBC	Total plate bacterial count

TVB-N	Total volatile basic nitrogen
TVC	Total viable count
WCA	Water contact angle
WVP	Water vapor permeability

## Author contributions

Ajitkumar Appayya Hunashyal: conceptualization, data interpretation, formal analysis, writing – original draft. Saraswati P. Masti: supervision, corresponding author, review, and manuscript corrections. Lingaraj Kariyappa Kurabetta: data curation, formal analysis. Manjushree Nagaraj Gunaki: study design, formal analysis, data curation, investigation. Suhasini Madihalli: data curation, formal analysis. Jennifer P. Pinto: conceptualization, data interpretation, review. Manjunath B. Megalamani: resource, manuscript corrections. Bothe Thokchom: antimicrobial and antioxidant studies. Ramesh Babu Yarajarla: resource, manuscript corrections. Ravindra B. Chougale: manuscript revision.

## Conflicts of interest

The authors declare no conflict of interest.

## Data availability

The data supporting the findings of this study are available from the corresponding author upon reasonable request.

Supplementary information: S1: TEM EDS and elemental mapping. S2: characterizations of NLCDs. S3: characterizations of nanocomposite film. S4: prawn packaging studies. S5: statistical analysis. See DOI: <https://doi.org/10.1039/d5fb00358j>.

## Acknowledgements

The authors are thankful to the Science and Engineering Research Board (SERB) for providing the instrumental facilities under the project sanctioned to Dr Saraswati P. Masti, Principal Investigator, SERB (Sanction Letter No. SB/EMEQ-213/2014 dated: 29-01-2016). We gratefully acknowledge the Sophisticated Analytical Instrumentation Facilities (SAIF), University Scientific and Instrumentation Centre (USIC), and DST-PURSE Phase II Program [Grant No. SR/PURSE PHASE-2/13(G)], Karnatak University, Dharwad, for providing necessary instrumentation support. Mr Ajitkumar Appayya Hunashyal extends his gratitude to KSTePS, Karnataka, India, for awarding a K-DST Research Fellowship.

## References

- 1 A. O. C. Iroegbu, S. S. Ray, V. Mbarane, J. C. Bordado and J. P. Sardinha, Plastic Pollution: A Perspective on Matters Arising: Challenges and Opportunities, *ACS Omega*, 2021, **6**(30), 19343–19355.
- 2 K. Kadac-Czapska, E. Knez, M. Gierszewska, E. Olewnik-Kruszkowska and M. Grembecka, Microplastics Derived from Food Packaging Waste—Their Origin and Health Risks, *Materials*, 2023, **16**(2), 674.



- 3 D. Allen, S. Allen, S. Abbasi, A. Baker, M. Bergmann, J. Brahney, *et al.*, Microplastics and nanoplastics in the marine-atmosphere environment, *Nat. Rev. Earth Environ.*, 2022, **3**(6), 393–405.
- 4 B. L. Tardy, J. J. Richardson, L. G. Greca, J. Guo, J. Bras and O. J. Rojas, Advancing bio-based materials for sustainable solutions to food packaging, *Nat. Sustain.*, 2022, **6**(4), 360–367.
- 5 R. Geyer, J. R. Jambeck and K. L. Law, Production, use, and fate of all plastics ever made, *Sci. Adv.*, 2017, **3**(7), DOI: [10.1126/sciadv.1700782](https://doi.org/10.1126/sciadv.1700782).
- 6 A. Matloob, H. Ayub, M. Mohsin, S. Ambreen, F. A. Khan, S. Oranab, *et al.*, A Review on Edible Coatings and Films: Advances, Composition, Production Methods, and Safety Concerns, *ACS Omega*, 2023, **8**(32), 28932–28944.
- 7 S. Davoodi, S. M. Davachi, A. G. Golkhajeh, A. S. Shekarabi and A. Abbaspourrad, Development and Characterization of *Salvia macrosiphon*/Chitosan Edible Films, *ACS Sustain. Chem. Eng.*, 2020, **8**(3), 1487–1496.
- 8 N. Tzortzakis and A. Chrysargyris, Postharvest ozone application for the preservation of fruits and vegetables, *Food Rev. Int.*, 2017, **33**(3), 270–315.
- 9 Y. Xin, M. Zhang, B. Xu, B. Adhikari and J. Sun, Research trends in selected blanching pretreatments and quick freezing technologies as applied in fruits and vegetables: a review, *Int. J. Refrig.*, 2015, **57**, 11–25.
- 10 V. Yemmireddy, A. Adhikari and J. Moreira, Effect of ultraviolet light treatment on microbiological safety and quality of fresh produce: an overview, *Front. Nutr.*, 2022, **9**, DOI: [10.3389/fnut.2022.871243](https://doi.org/10.3389/fnut.2022.871243).
- 11 M. Giannoglou, Z. M. Xanthou, S. Chanioti, P. Stergiou, M. Christopoulos, P. Dimitrakellis, *et al.*, Effect of cold atmospheric plasma and pulsed electromagnetic fields on strawberry quality and shelf-life, *Innov. Food Sci. Emerg. Technol.*, 2021, **68**, 102631.
- 12 R. Priyadarshi, F. Deeba, Sauraj and Y. S. Negi, Modified atmosphere packaging development, in *Processing and Development of Polysaccharide-Based Biopolymers for Packaging Applications*, Elsevier, 2020, pp. 261–280.
- 13 P. Ezati, R. Priyadarshi, Y. J. Bang and J. W. Rhim, CMC and CNF-based intelligent pH-responsive color indicator films integrated with shikonin to monitor fish freshness, *Food Control*, 2021, **126**, 108046.
- 14 P. Ezati, Y. J. Bang and J. W. Rhim, Preparation of a shikonin-based pH-sensitive color indicator for monitoring the freshness of fish and pork, *Food Chem.*, 2021, **337**, 127995.
- 15 P. Ezati, Z. Riahi and J. W. Rhim, Carrageenan-Based Functional Films Integrated with CuO-Doped Titanium Nanotubes for Active Food-Packaging Applications, *ACS Sustain. Chem. Eng.*, 2021, **9**(28), 9300–9307.
- 16 S. Davoodi, S. M. Davachi, A. G. Golkhajeh, A. S. Shekarabi and A. Abbaspourrad, Development and Characterization of *Salvia macrosiphon*/Chitosan Edible Films, *ACS Sustain. Chem. Eng.*, 2020, **8**(3), 1487–1496.
- 17 S. Roy, P. Ezati and J. W. Rhim, Gelatin/Carrageenan-Based Functional Films with Carbon Dots from Enoki Mushroom for Active Food Packaging Applications, *ACS Appl. Polym. Mater.*, 2021, **3**(12), 6437–6445.
- 18 P. Ezati, H. Tajik and M. Moradi, Fabrication and characterization of alizarin colorimetric indicator based on cellulose-chitosan to monitor the freshness of minced beef, *Sens. Actuators, B*, 2019, **285**, 519–528.
- 19 P. Ezati, H. Tajik, M. Moradi and R. Molaei, Intelligent pH-sensitive indicator based on starch-cellulose and alizarin dye to track freshness of rainbow trout fillet, *Int. J. Biol. Macromol.*, 2019, **132**, 157–165.
- 20 S. Cailotto, E. Amadio, M. Facchin, M. Selva, E. Pontoglio, F. Rizzolio, *et al.*, Carbon Dots from Sugars and Ascorbic Acid: Role of the Precursors on Morphology, Properties, Toxicity, and Drug Uptake, *ACS Med. Chem. Lett.*, 2018, **9**(8), 832–837.
- 21 R. Wang, K. Q. Lu, Z. R. Tang and Y. J. Xu, Recent progress in carbon quantum dots: synthesis, properties and applications in photocatalysis, *J. Mater. Chem. A*, 2017, **5**(8), 3717–3734.
- 22 O. Kozák, M. Sudolská, G. Pramanik, P. Cígler, M. Otyepka and R. Zbořil, Photoluminescent Carbon Nanostructures, *Chem. Mater.*, 2016, **28**(12), 4085–4128.
- 23 A. Anand, B. Unnikrishnan, S. C. Wei, C. P. Chou, L. Z. Zhang and C. C. Huang, Graphene oxide and carbon dots as broad-spectrum antimicrobial agents – a minireview, *Nanoscale Horiz.*, 2019, **4**(1), 117–137.
- 24 F. Yan, Y. Jiang, X. Sun, Z. Bai, Y. Zhang and X. Zhou, Surface modification and chemical functionalization of carbon dots: a review, *Microchim. Acta*, 2018, **185**(9), 424.
- 25 B. Yao, H. Huang, Y. Liu and Z. Kang, Carbon Dots: A Small Conundrum, *Trends Chem.*, 2019, **1**(2), 235–246.
- 26 J. Wang and J. Qiu, A review of carbon dots in biological applications, *J. Mater. Sci.*, 2016, **51**(10), 4728–4738.
- 27 C. Murru, R. Badía-Laíño and M. E. Díaz-García, Synthesis and Characterization of Green Carbon Dots for Scavenging Radical Oxygen Species in Aqueous and Oil Samples, *Antioxidants*, 2020, **9**(11), 1147.
- 28 T. Tong, H. Hu, J. Zhou, S. Deng, X. Zhang, W. Tang, *et al.*, Glycyrrhizic-Acid-Based Carbon Dots with High Antiviral Activity by Multisite Inhibition Mechanisms, *Small*, 2020, **16**(13), DOI: [10.1002/sml.201906206](https://doi.org/10.1002/sml.201906206).
- 29 K. L. Deepika and K. K. Gaikwad, Carbon dots for food packaging applications, *Sustainable Food Technol.*, 2023, **1**(2), 185–199.
- 30 X. Luo, Y. Han, X. Chen, W. Tang, T. Yue and Z. Li, Carbon dots derived fluorescent nanosensors as versatile tools for food quality and safety assessment: a review, *Trends Food Sci. Technol.*, 2020, **95**, 149–161.
- 31 I. B. Basumatary, A. Mukherjee, V. Katiyar and S. Kumar, Biopolymer-based nanocomposite films and coatings: recent advances in shelf-life improvement of fruits and vegetables, *Crit. Rev. Food Sci. Nutr.*, 2022, **62**(7), 1912–1935.
- 32 A. A. Oun, G. H. Shin, J. W. Rhim and J. T. Kim, Recent advances in polyvinyl alcohol-based composite films and their applications in food packaging, *Food Packag. Shelf Life*, 2022, **34**, 100991.



- 33 M. N. Gunaki, S. P. Masti, L. K. Kurabetta, S. Madihalli, A. A. Hunashyal, R. B. Chougale, *et al.*, Chitosan-encapsulated CuO nanoparticles reinforced multifunctional chitosan/gelatine nanocomposite films: a promising extension of cherry and grape shelf life, *J. Environ. Chem. Eng.*, 2025, **13**(5), 118397.
- 34 M. N. Gunaki, S. P. Masti, L. K. Kurabetta, J. P. Pinto, A. A. Hunashyal, N. P. Dalbhanjan, *et al.*, Influence of chitosan-capped quercetin nanoparticles on chitosan/poly(vinyl) alcohol multifunctional films: a sustainable approach for bread preservation, *Int. J. Biol. Macromol.*, 2025, **299**, 140029.
- 35 L. K. Kurabetta, S. P. Masti, M. P. Eelager, M. N. Gunaki, S. Madihalli, A. A. Hunashyal, *et al.*, Physicochemical and antioxidant properties of tannic acid crosslinked cationic starch/chitosan based active films for ladyfinger packaging application, *Int. J. Biol. Macromol.*, 2023, **253**, 127552.
- 36 S. Madihalli, S. P. Masti, M. P. Eelager, R. B. Chougale, L. K. Kurabetta, A. A. Hunashyal, *et al.*, Quinic acid and montmorillonite integrated chitosan/pullulan active films with potent antimicrobial and barrier properties to prolong the shelf life of tofu, *Food Biosci.*, 2024, **62**, 105492.
- 37 J. P. Pinto, O. J. D'souza, C. Chavan, R. F. Bhajanthri, S. P. Masti and R. B. Chougale, Tuning the energy storage performance of graphene oxide-based nanocomposite films by encapsulating silver nanoparticles, *Diam. Relat. Mater.*, 2023, **140**, 110483.
- 38 J. P. Pinto, M. H. Anandalli, A. A. Hunashyal, H. Priyadarshini, S. P. Masti, R. B. Chougale, *et al.*, Carbon nanotubes reinforced chitosan/poly (1-vinylpyrrolidone-co-vinyl acetate) films: a sustainable approach for optoelectronic applications, *J. Mater. Sci.: Mater. Electron.*, 2025, **36**(17), 1035.
- 39 M. Jridi, S. Hajji, H. B. Ayed, I. Lassoued, A. Mbarek, M. Kammoun, *et al.*, Physical, structural, antioxidant and antimicrobial properties of gelatin-chitosan composite edible films, *Int. J. Biol. Macromol.*, 2014, **67**, 373–379.
- 40 Y. Liu, S. Wang and R. Zhang, Composite poly(lactic acid)/chitosan nanofibrous scaffolds for cardiac tissue engineering, *Int. J. Biol. Macromol.*, 2017, **103**, 1130–1137.
- 41 L. K. Kurabetta, S. P. Masti, M. N. Gunaki, A. A. Hunashyal, R. B. Chougale, N. P. Dalbhanjan, *et al.*, Vanillin reinforced cationic starch/poly(vinyl alcohol) based antimicrobial and antioxidant bioactive films: sustainable food packaging materials, *Sustainable Food Technol.*, 2025, 1353–1364.
- 42 V. Gudihal, R. F. Bhajanthri, C. Chavan, N. K. H., J. P. Pinto and Y. Patil, Synergistic Influence of ZnO Nanofillers and Sodium Alginate on Ionic Transport in PVA/NaCMC Polymer Electrolytes for Primary Battery Systems, *Research Square*, 2025, DOI: [10.21203/rs.3.rs-7201607/v1](https://doi.org/10.21203/rs.3.rs-7201607/v1).
- 43 M. P. Eelager, S. P. Masti, S. Madihalli, N. Gouda, L. K. Kurabetta, M. N. Gunaki, *et al.*, The effect of cetrinide crosslinking on biodegradable PVA/xanthan gum herbicidal films: towards sustainable agriculture and its influence on soil fertility, *J. Environ. Chem. Eng.*, 2025, **13**(2), 116029.
- 44 L. K. Kurabetta, S. P. Masti, M. N. Gunaki, A. A. Hunashyal, R. B. Chougale, N. P. Dalbhanjan, *et al.*, Exploration of physicochemical and biological properties of phenylalanine incorporated carboxymethyl cellulose/poly(vinyl alcohol) based bioactive films for food packaging applications, *Food Biosci.*, 2024, **61**, 104869.
- 45 M. N. V. Ravi Kumar, A review of chitin and chitosan applications, *React. Funct. Polym.*, 2000, **46**(1), 1–27.
- 46 A. Giannakas, M. Vlachas, C. Salmas, A. Leontiou, P. Katapodis, H. Stamatis, *et al.*, Preparation, characterization, mechanical, barrier and antimicrobial properties of chitosan/PVOH/clay nanocomposites, *Carbohydr. Polym.*, 2016, **140**, 408–415.
- 47 H. Wang, R. Zhang, H. Zhang, S. Jiang, H. Liu, M. Sun, *et al.*, Kinetics and functional effectiveness of nisin loaded antimicrobial packaging film based on chitosan/poly(vinyl alcohol), *Carbohydr. Polym.*, 2015, **127**, 64–71.
- 48 H. Wang, J. Qian and F. Ding, Emerging Chitosan-Based Films for Food Packaging Applications, *J. Agric. Food Chem.*, 2018, **66**(2), 395–413.
- 49 S. Liang, X. Wang, C. Wei, L. Xie, Z. Song and X. Dang, Corrigendum to “Remediation and resource utilization of Cr(III), Al(III) and Zr(IV)-containing tannery effluent based on chitosan-carboxymethyl cellulose aerogel” [Journal of Bioresources and Bioproducts, 10 (2025) 77-91], *J. Bioresour. Bioprod.*, 2025, **10**(3), 425–426.
- 50 X. Dang, S. Han, Y. Du, Y. Fei, B. Guo and X. Wang, Engineered environment-friendly multifunctional food packaging with superior nonleachability, polymer miscibility and antimicrobial activity, *Food Chem.*, 2025, **466**, 142192.
- 51 X. Dang, Y. Cai and X. Wang, An all-natural strategy for versatile biomass-based active food packaging film with superior biodegradability, antioxidant and antimicrobial activity, *Food Chem.*, 2025, **480**, 143922.
- 52 X. Dang, S. Han and X. Wang, Versatile corn starch-based sustainable food packaging with enhanced antimicrobial activity and preservative properties, *J. Colloid Interface Sci.*, 2025, **694**, 137698.
- 53 S. Liang, X. Wang, C. Wei, L. Xie and X. Dang, Engineering a Natural Multifunctional Biomass-Based Composite Nanosystem for Active Smart Packaging and Colorimetric Labels, *ACS Sustain. Chem. Eng.*, 2025, **13**(8), 3066–3077.
- 54 S. Roy, P. Ezati and J. W. Rhim, Gelatin/Carrageenan-Based Functional Films with Carbon Dots from Enoki Mushroom for Active Food Packaging Applications, *ACS Appl. Polym. Mater.*, 2021, **3**(12), 6437–6445.
- 55 L. K. Kurabetta, S. P. Masti, M. N. Gunaki, A. A. Hunashyal, M. P. Eelager, R. B. Chougale, *et al.*, A synergistic influence of gallic acid/ZnO NPs to strengthen the multifunctional properties of methylcellulose: a conservative approach for tomato preservation, *Int. J. Biol. Macromol.*, 2024, **277**, 134191.
- 56 B. Thokchom, S. M. Bhavi, M. B. Abbigeri, A. K. Shettar and R. B. Yarajarla, Green synthesis, characterization and



- biomedical applications of *Centella asiatica*-derived carbon dots, *Carbon Lett.*, 2023, **33**(4), 1057–1071.
- 57 S. M. Bhavi, B. Thokchom, M. B. Abbigeri, S. S. Bhat, S. R. Singh, P. Joshi, *et al.*, Green synthesis, characterization, antidiabetic, antioxidant and antibacterial applications of silver nanoparticles from *Syzygium caryophyllatum* (L.) Alston leaves, *Process Biochem.*, 2024, **145**, 89–103.
- 58 J. P. Pinto, V. D. Hiremani, O. J. D'souza, S. Khanapure, S. S. Narasagoudr, N. Goudar, *et al.*, Development of Chitosan-Copovidone nanocomposite films with antioxidant and antibacterial properties for food packaging applications, *Food Humanity*, 2023, **1**, 378–390.
- 59 A. Khan, P. Ezati and J. W. Rhim, Chitosan/Starch-Based Active Packaging Film with N, P-Doped Carbon Dots for Meat Packaging, *ACS Appl. Bio Mater.*, 2023, **6**(3), 1294–1305.
- 60 R. Kumar, H. S. Mavi and A. K. Shukla, Spectroscopic Investigation of Quantum Confinement Effects in Ion Implanted Silicon-on-Sapphire Films, *Silicon*, 2010, **2**(1), 25–31.
- 61 S. K. Saxena, P. Yogi, S. Mishra, H. M. Rai, V. Mishra, M. K. Warshi, *et al.*, Amplification or cancellation of Fano resonance and quantum confinement induced asymmetries in Raman line-shapes, *Phys. Chem. Chem. Phys.*, 2017, **19**(47), 31788–31795.
- 62 K. Jlassi, K. Eid, M. H. Sliem, A. M. Abdullah, M. M. Chehimi and I. Krupa, Rational synthesis, characterization, and application of environmentally friendly (polymer-carbon dot) hybrid composite film for fast and efficient UV-assisted Cd<sup>2+</sup> removal from water, *Environ. Sci. Eur.*, 2020, **32**(1), 12.
- 63 T. Boobalan, M. Sethupathi, N. Sengottuvelan, P. Kumar, P. Balaji, B. Gulyás, *et al.*, Mushroom-Derived Carbon Dots for Toxic Metal Ion Detection and as Antibacterial and Anticancer Agents, *ACS Appl. Nano Mater.*, 2020, **3**(6), 5910–5919.
- 64 J. Liu, R. Li and B. Yang, Carbon Dots: A New Type of Carbon-Based Nanomaterial with Wide Applications, *ACS Cent. Sci.*, 2020, **6**(12), 2179–2195.
- 65 A. S. Mathad, J. Seetharamappa and S. S. Kalanur,  $\beta$ -Cyclodextrin anchored neem carbon dots for enhanced electrochemical sensing performance of an anticancer drug, lapatinib via host-guest inclusion, *J. Mol. Liq.*, 2022, **350**, 118582.
- 66 G. Gedda, S. A. Sankaranarayanan, C. L. Putta, K. K. Gudimella, A. K. Rengan and W. M. Girma, Green synthesis of multi-functional carbon dots from medicinal plant leaves for antimicrobial, antioxidant, and bioimaging applications, *Sci. Rep.*, 2023, **13**(1), 6371.
- 67 R. Sandhir, M. Khurana and N. K. Singhal, Potential benefits of phytochemicals from *Azadirachta indica* against neurological disorders, *Neurochem. Int.*, 2021, **146**, 105023.
- 68 P. K. Yadav, V. K. Singh, S. Chandra, D. Bano, V. Kumar, M. Talat, *et al.*, Green Synthesis of Fluorescent Carbon Quantum Dots from *Azadirachta indica* Leaves and Their Peroxidase-Mimetic Activity for the Detection of H<sub>2</sub>O<sub>2</sub> and Ascorbic Acid in Common Fresh Fruits, *ACS Biomater. Sci. Eng.*, 2019, **5**(2), 623–632.
- 69 P. Ezati, Z. Riahi and J. W. Rhim, Carrageenan-Based Functional Films Integrated with CuO-Doped Titanium Nanotubes for Active Food-Packaging Applications, *ACS Sustain. Chem. Eng.*, 2021, **9**(28), 9300–9307.
- 70 S. F. Hosseini, M. Rezaei, M. Zandi and F. Farahmandghavi, Fabrication of bio-nanocomposite films based on fish gelatin reinforced with chitosan nanoparticles, *Food Hydrocoll.*, 2015, **44**, 172–182.
- 71 J. Ahmad, K. Deshmukh and M. B. Hägg, Influence of TiO<sub>2</sub> on the Chemical, Mechanical, and Gas Separation Properties of Polyvinyl Alcohol-Titanium Dioxide (PVA-TiO<sub>2</sub>) Nanocomposite Membranes, *Int. J. Polym. Anal. Charact.*, 2013, **18**(4), 287–296.
- 72 S. Jiang, C. Qiao, R. Liu, Q. Liu, J. Xu and J. Yao, Structure and properties of citric acid cross-linked chitosan/poly(vinyl alcohol) composite films for food packaging applications, *Carbohydr. Polym.*, 2023, **312**, 120842.
- 73 X. Zhang, H. Wang, N. Niu, Z. Chen, S. Li, S. X. Liu, *et al.*, Fluorescent Poly(vinyl alcohol) Films Containing Chlorogenic Acid Carbon Nanodots for Food Monitoring, *ACS Appl. Nano Mater.*, 2020, **3**(8), 7611–7620.
- 74 A. Konwar, N. Gogoi, G. Majumdar and D. Chowdhury, Green chitosan-carbon dots nanocomposite hydrogel film with superior properties, *Carbohydr. Polym.*, 2015, **115**, 238–245.
- 75 Y. You, H. Zhang, Y. Liu and B. Lei, Transparent sunlight conversion film based on carboxymethyl cellulose and carbon dots, *Carbohydr. Polym.*, 2016, **151**, 245–250.
- 76 M. Sultan, A. Youssef and R. A. Baseer, Fabrication of multifunctional ZnO@tannic acid nanoparticles embedded in chitosan and polyvinyl alcohol blend packaging film, *Sci. Rep.*, 2024, **14**(1), 18533.
- 77 Y. Du and M. Zheng, Silver nanoparticles/carbon dots nanocomposite with potent antibiofilm and long-term antimicrobial activity doped into chitosan/polyvinyl alcohol film for food preservation, *Int. J. Biol. Macromol.*, 2024, **283**, 137744.
- 78 A. Khan, R. Priyadarshi, T. Bhattacharya and J. W. Rhim, Carrageenan/Alginate-Based Functional Films Incorporated with *Allium sativum* Carbon Dots for UV-Barrier Food Packaging, *Food Bioprocess Technol.*, 2023, **16**(9), 2001–2015.
- 79 A. Khan, R. Priyadarshi, T. Bhattacharya and J. W. Rhim, Carrageenan/Alginate-Based Functional Films Incorporated with *Allium sativum* Carbon Dots for UV-Barrier Food Packaging, *Food Bioprocess Technol.*, 2023, **16**(9), 2001–2015.
- 80 N. Khazaei, M. Esmaili, Z. E. Djomeh, M. Ghasemlou and M. Jouki, Characterization of new biodegradable edible film made from basil seed (*Ocimum basilicum* L.) gum, *Carbohydr. Polym.*, 2014, **102**, 199–206.
- 81 M. Jouki, F. T. Yazdi, S. A. Mortazavi and A. Koocheki, Physical, barrier and antioxidant properties of a novel



- plasticized edible film from quince seed mucilage, *Int. J. Biol. Macromol.*, 2013, **62**, 500–507.
- 82 M. Jouki, N. Khazaei and A. Jouki, Fabrication and characterization of an active biodegradable edible packaging film based on sesame seed gum (*Sesamum indicum* L.), *J. Food Meas. Char.*, 2021, **15**(5), 4748–4757.
- 83 M. Ö. Alaş, G. Doğan, M. S. Yalcin, S. Ozdemir and R. Genç, Multicolor Emitting Carbon Dot-Reinforced PVA Composites as Edible Food Packaging Films and Coatings with Antimicrobial and UV-Blocking Properties, *ACS Omega*, 2022, **7**(34), 29967–29983.
- 84 P. Ezati, J. W. Rhim, R. Molaei and Z. Rezaei, Carbon quantum dots-based antifungal coating film for active packaging application of avocado, *Food Packag. Shelf Life*, 2022, **33**, 100878.
- 85 A. Hameed, T. U. Rehman, Z. A. Rehan, R. Noreen, S. Iqbal, S. Batool, *et al.*, Development of polymeric nanofibers blended with extract of neem (*Azadirachta indica*), for potential biomedical applications, *Front. Mater.*, 2022, **9**, DOI: [10.3389/fmats.2022.1042304](https://doi.org/10.3389/fmats.2022.1042304).
- 86 P. Das, S. Ganguly, S. R. Ahmed, M. Sherazee, S. Margel, A. Gedanken, *et al.*, Carbon Dot Biopolymer-Based Flexible Functional Films for Antioxidant and Food Monitoring Applications, *ACS Appl. Polym. Mater.*, 2022, **4**(12), 9323–9340.
- 87 D. Wang, X. Wang, S. Zhou, L. Ren, Y. Meng, R. Ma, *et al.*, Radish residue carbon dots-based novel starch/chitosan film with high antioxidant, biocompatibility, and antibacterial activities for salmon fillets' active packaging, *Int. J. Biol. Macromol.*, 2024, **273**, 133107.
- 88 W. Gao, B. Mu, F. Yang, Y. Li, X. Wang and A. Wang, Multifunctional honeysuckle extract/attapulgitic/chitosan composite films containing natural carbon dots for intelligent food packaging, *Int. J. Biol. Macromol.*, 2024, **280**, 136042.
- 89 F. Garavand, I. Cacciotti, N. Vahedikia, A. Rehman, Ö. Tarhan, S. Akbari-Alavijeh, *et al.*, A comprehensive review on the nanocomposites loaded with chitosan nanoparticles for food packaging, *Crit. Rev. Food Sci. Nutr.*, 2022, **62**(5), 1383–1416.
- 90 X. Dang, N. Li, Z. Yu, X. Ji, M. Yang and X. Wang, Advances in the preparation and application of cellulose-based antimicrobial materials: A review, *Carbohydr. Polym.*, 2024, **342**, 122385.
- 91 X. Dang, S. Han, J. Tang and X. Wang, Functional Starch-Based Conductive Hydrogel for Flexible Electronics: Design, Construction, and Applications, *Aggregate*, 2025, DOI: [10.1002/agt2.70121](https://doi.org/10.1002/agt2.70121).
- 92 F. Norouzi, M. Pourmadadi, F. Yazdian, K. Khoshmaram, J. Mohammadnejad, M. H. Sanati, *et al.*, PVA-Based Nanofibers Containing Chitosan Modified with Graphene Oxide and Carbon Quantum Dot-Doped TiO<sub>2</sub> Enhance Wound Healing in a Rat Model, *J. Funct. Biomater.*, 2022, **13**(4), 300.
- 93 P. E. F. Melo, A. O. da Silva, K. W. E. Miranda, P. M. de Farias, B. Iles, W. da Silva Reatgui, *et al.*, Chitosan and polyvinyl alcohol nanocomposite incorporated with carbon dots: a proposal for packaging, *Polymer*, 2025, **334**, 128755.
- 94 C. Li, J. Liu, W. Li, Z. Liu, X. Yang, B. Liang, *et al.*, Biobased Intelligent Food-Packaging Materials with Sustained-Release Antibacterial and Real-Time Monitoring Ability, *ACS Appl. Mater. Interfaces*, 2023, **15**(31), 37966–37975.
- 95 Z. Yu, B. Li, J. Chu and P. Zhang, Silica in situ enhanced PVA/chitosan biodegradable films for food packages, *Carbohydr. Polym.*, 2018, **184**, 214–220.
- 96 A. A. Shah, F. Hasan, A. Hameed and S. Ahmed, Biological degradation of plastics: a comprehensive review, *Biotechnol. Adv.*, 2008, **26**(3), 246–265.
- 97 M. Zhu, D. Ying, H. Zhang, X. Xu and C. Chang, Self-healable hydrophobic films fabricated by incorporating natural wax into cellulose matrix, *Chem. Eng. J.*, 2022, **446**, 136791.
- 98 H. Long, J. Gu, J. Jiang, L. Guan, X. Lin, W. Zhang, *et al.*, Mechanically strong and biodegradable holocellulose films prepared from *Camellia oleifera* shells, *Carbohydr. Polym.*, 2023, **299**, 120189.
- 99 A. Susmitha, K. Sasikumar, D. Rajan, M. A. Padmakumar and K. M. Nampoothiri, Development and characterization of corn starch-gelatin based edible films incorporated with mango and pineapple for active packaging, *Food Biosci.*, 2021, **41**, 100977.
- 100 M. Aider, Chitosan application for active bio-based films production and potential in the food industry: Review, *LWT-Food Sci. Technol.*, 2010, **43**(6), 837–842.
- 101 G. Murugan, A. Khan, K. Nilswan, J. T. Kim, S. Benjakul and J. W. Rhim, Chitosan/Polyvinyl Alcohol Based Blend Film Containing Tangerine Peel Carbon Dots: Properties, Antioxidant and Antibacterial Activities, *Waste Biomass Valorization*, 2024, **19**, 2255–2270.
- 102 M. B. Priyadarshini, R. K. Majumder and P. Maurya, Effect of vacuum packaging on the shelf-life of shrimp analog prepared from *Pangasionodon hypophthalmus* surimi during refrigerated storage, *J. Food Process. Preserv.*, 2022, **46**(3), DOI: [10.1111/jfpp.16369](https://doi.org/10.1111/jfpp.16369).
- 103 J. S. Simoes, E. T. Mársico, C. A. L. De La Torre, S. B. Mano, R. M. Franco, L. F. L. D. Santos, *et al.*, Nutritional and Sensory Quality of the Freshwater Prawn *Macrobrachium rosenbergii* and the Influence of Packaging Permeability on its Shelf Life, *J. Aquat. Food Prod. Technol.*, 2019, **28**(6), 703–714.
- 104 L. Wei, H. Yuanyuan, C. Yanping, J. Jiaojiao and H. Guohua, *Penaeus orientalis* prawn freshness rapid determination method based on electronic nose and non-linear stochastic resonance technique, *Bioengineered*, 2015, **6**(1), 42–52.
- 105 A. E. D. A. Bekhit, B. W. B. Holman, S. G. Giteru and D. L. Hopkins, Total volatile basic nitrogen (TVB-N) and its role in meat spoilage: a review, *Trends Food Sci. Technol.*, 2021, **109**, 280–302.
- 106 S. Hu, W. Feng, H. Jiang and J. Chen, A Chitosan-Based Dual-Functional Packaging Film Integrated Carbon Dots with Enhanced pH Sensing Ability for Fish Freshness



- Monitoring and Maintenance, *Food Bioprocess Technol.*, 2024, **18**, 3484–3503.
- 107 L. Wei, H. Yuanyuan, C. Yanping, J. Jiaojiao and H. Guohua, *Penaeus orientalis* prawn freshness rapid determination method based on electronic nose and non-linear stochastic resonance technique, *Bioengineered*, 2015, **6**(1), 42–52.
- 108 T. D. Thangadurai, N. Manjubaashini, A. Sowndarya, A. Subitha, G. Kausalya, S. Shanmugaraju, *et al.*, Multipurpose biological applications of excitation-dependent fluorescent carbon nano dots emanated from biomass waste, *Mater. Chem. Phys.*, 2023, **307**, 128113.
- 109 T. Liu, L. Jiang, Y. Wang, M. Li, Z. Li and Y. Liu, Bilayer pH-sensitive colorimetric indicator films based on chitosan/purple carrot extract and gellan gum/Mg-carbon dots for visual monitoring of pork freshness, *Food Packag. Shelf Life*, 2024, **45**, 101336.
- 110 M. I. Hidayat, A. Hardiansyah, K. Khoiriah, E. Yulianti, R. A. K. Wardhani, F. Fahrialdi, *et al.*, Composite films based on chitosan incorporating molybdenum disulfide nanosheets and zinc oxide nanoparticles with potential antibacterial application, *Food Chem.*, 2025, **477**, 143480.
- 111 N. P. Dalbanjan, M. P. Eelager, K. Korgaonkar, B. N. Gonal, A. J. Kadapure, S. B. Arakera, *et al.*, Descriptive review on conversion of waste residues into valuable bionanocomposites for a circular bioeconomy, *Nano-Struct. Nano-Objects*, 2024, **39**, 101265.
- 112 A. B. Kharissova, O. V. Kharissova, B. I. Kharisov and Y. P. Méndez, Carbon negative footprint materials: a review, *Nano-Struct. Nano-Objects*, 2024, **37**, 101100.

